P A R T   I I I

MICROHARDNESS AND ELECTRICAL CONDUCTIVITY OF

CALCITE AND POTASSIUM CHLORIDE (PURE AND DOPED)

CRYSTALS

CHAPTER VII

MICROHARDNESS OF CRYSTALS (GENERAL)

CHAPTER VII

MICROHARDNESS OF CRYSTALS (GENERAL)

7.1 INTRODUCTION:

Hardness may be broadly defined as the ability of one body to resist penetration by another. It is by definition a relative property of a material and depends on the elastic and plastic properties of both the penetrated body and the penetrator. In addition, the comparative hardness of different materials is strongly dependent upon the method of measurement, the four most general methods being (i) Scratch (ii) Indentation (iii) Abrasive and (iv) Dynamic methods. All hardness tests measure some combination of various

material properties, namely elastic modulus, yield

stress (which denotes the onset of plastic behaviour

or permanent distortion), physical imperfection,

impurities, and work-hardening capacity. The latter

is a measure of the increase in stress to continue

plastic flow as strain increases. Since each hardness

test measures a different combination of these properties,

hardness itself is not an absolute quantity and, to be

meaningful, any statement of the hardness of a body must

include the method used for measurements.

7.2   DEFINITIONS AND MEASUREMENTS:

From time to time many definitions have been

given for hardness but none has been found to be

satisfactory for quantitative interpretation of the

processes taking place in indented materials. Tuckerman

(1929) explained hardness as a hazily conceived aggregate

or conglomeration of properties of a material more or

less related to each other. Best general definition is

given by Ashby (1951), "Hardness is a measure of the

resistance to permanent deformation or damage". The

general definition of indentation hardness which relates

to the various forms of the indenters is the ratio of

load applied to the surface area of the indentation.
Mayer (1908) proposed that hardness should be defined
as the ratio of the load to the projected area of the
indentation. So the hardness has the dimension of stress.
Spaeth (1940) suggested that hardness should not be
defined as stress but as the resistance to indentation
in the form of the ratio of the specific surface load·
to the unrecovered deformation. In short, the hardness
of a solid is defined by the resistance against lattice
destruction and is considered to be a function of inter
atomic forces (Tertsch, 1948). Attempts towards a
physical definition of hardness were made by Friedrich
(1926), Goldschmidt (1927) and Chatterjee (1954).

Chatterjee (1954) defined indentation hardness
as the work done ·per unit volume of the indentation in
a static indentation test for a definite angle of
indentation. On the basis of this definition and Meyer's
law $P = ad^n$ for spherical indenters, he derived a formula
for the measurement of hardness. According to Plendl
and Gielisse (1962) hardness can be defined as pressure
or force per square centimeter, and thus it can be conceived
as an energy per unit volume e.g. the ratio between the

input energy and volume of indentation. They have
concluded that resistance is a function of the lattice
energy per unit volume and called it volumetric lattice
energy (U/V) having the dimension ergs/cm^3. U is the
total cohesive energy of the lattice per mole and V
is the molecular volume defined as M/S, where M is a
molecular weight and S is specific heat. The hardness
was thus considered to be the absolute overall hardness.
Matkin and Caffyn (1963) from their studies on hardness
of sodium chloride single crystals containing divalent
impurities, correlated hardness with the dislocation
theory. They redefined hardness in terms of generation
and/or movement of dislocations associated with indentation,
or it is the measure of the rate at which the dislocations
dissipate energy when moving through a crystal lattice.

There are basically four different methods to
determine hardness of a substance. (1) Scratch (2) Abrasive
(3) Dynamic (4) Static indentation method.

(1) Scratch Hardness:
An early method of measuring scratch hardness
still in wide use today by mineralogists was developed
by Friedrich Mohs in (1822). This gives a relative

ranking of minerals based simply on their ability to scratch one another. The Mohs method is not suitable for general use with materials of hardness greater than 4, since in this range the intervals are rather closely and unevenly spaced. The modifications of this method were overshadowed by other sensitive methods and experiments.

(2) Abrasive Hardness:

Abrasive hardness is defined as the resistance to mechanical wear, a measure of which is the amount of material removed from the surface under specific conditions. The hardness may be found by the depth of penetration. For ferromagnetic materials hardness measurements have been made with attempts to associate them with the magnetic properties. It is generally found that materials with large magnetic coercive force are mechanically deformed to a greater extent than the material with less magnetic coercive force. It is found that hardness varies generally in the same way as the electrical resistivity.

(3) Dynamic Hardness:

The hardness measurement in this method involves the dynamic deformation of specimen under study and is
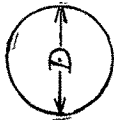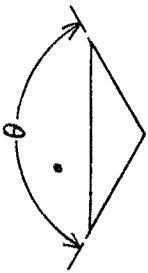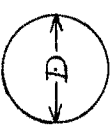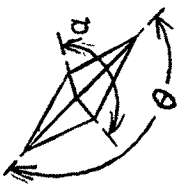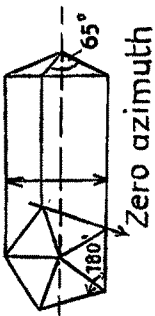
determined by following different considerations:

(a) Here a steel sphere or a diamond-tipped hammer is dropped from a given height, and the height to which the ball or hammer rebounds is read on a scale. This is taken to be the measure of hardness. The kinetic energy of the ball or hammer is used up partly in plastically deforming the specimen surface by creating a slight impression and partly in the rebound. This test is sometimes referred to as 'dynamic rebound test'.

(b) Here a steel sphere or diamond-tipped hammer is dropped from a given height, the depth and size of the impression produced and the energy of the impact gives the hardness of the substance, i.e. hardness is given as ratio of the energy of impact to the volume of indentation mark. (c) Chalmers (1941) assessed the surface hardness in terms of the reduction in optical reflectivity when a known amount of sand was allowed to impinge on the surface under standard conditions.

(4) Static Indentation Hardness:

The most widely used method of hardness testing is the indentation method. This is the simplest and a very sensitive method in which a hard indenter (e.g.

	Brinell	Rockwell	Vickers	Knoop	Brookes & Moxley
Material of which indenter is made	Hardened steel or tungston carbide	Diamond	Hardened steel	Diamond	Diamond	Diamond
Shape of indenter	Sphere	Cone	Sphere	Square based pyramid	Rhomb based pyramid	Pentagonal
Dimensions of indenter	$D = 10mm$	$\theta = 120°$	$D = \begin{cases} \frac{1}{16} \text{ in.} \\ \frac{1}{8} \text{ in.} \\ \frac{1}{4} \text{ in.} \\ \frac{1}{2} \text{ in.} \end{cases}$	$\theta = 136°$	$\alpha = 130°$ $\theta = 172°30'$	
Characteristics	1. Geometrically similar impressions are not obtained.	1. Prepares the surface upon which the further penetration due to major load is based. 2. Hardness is read directly on the dial gauge. 3. Hardness value may be appreciable in error due to large amount of recovery along depth.	1. Geometrically similar impressions are obtained	1. Hardness of upper most surface layers can be found. 2. Sensitive to anisotropy of crystals. 3. Shorter diagonal undergoes recovery.	1. Eliminates the anisotropy normally observed in hardness with all other indenters.

Brinell: Diagram of sphere with D dimension.

Rockwell: Diagram of cone with θ angle; also sphere with D.

Vickers: Square based pyramid diagram with $\theta = 136°$.

Knoop: Rhomb based pyramid diagram with α and θ angles.

Brookes & Moxley: Pentagonal indenter diagram with 65°, 180°, Zero azimuth.

diamond, sapphire, quartz or hardened steel) of a particular geometry is applied slowly, and after a certain time of application, is carefully removed, leaving behind a permanent indentation mark on the surface of the specimen. Measurement is made either of the size of the indentation resulting from a fixed load on the indenter or the load necessary to force the indenter down to a predetermined depth and the hardness of material is then defined as the ratio of the load to the area of the indent mark. The hardness values so obtained vary with indenter geometry and with the method of calculations.

Many combinations of indenter, load, loading procedure, and means of indentation measurement are used among the various tests in order to accommodate various shapes, sizes and hardnesses of specimens, and this has resulted in a proliferation of hardness scales. The most commonly used indenters are described in Table 7.1. Diamond indenters must be used for hard materials in order to minimize errors due to elastic distortion of the indenter. In case ball indenters are used, the hardness number will be independent of

load only when the ratio of load to indenter diameter
is held constant. For a cone and pyramid indenters,
hardness number will be independent of load for all
loads above a certain minimum depending upon the specimen
material.

7.3   GENERAL INFORMATION ON HARDNESS:

The hardness study undertaken, so far for
studying the strength of solids and the effect of various
treatments on the hardness of a solid, have proved some-
what useful. Most of the work has been reported on alkali
halides and metals. Previously, the hardness studies
were made only from the view of material research but as
the expansion in the field of scientific research increased,
the study on hardness helped in understanding various
oether mechanical properties of solids. Gilman and
Roberts (1961) correlated indentation hardness with the
elastic modulus by gathering the data for various materials.
Their empirical linear relation shows that elastic modulus
is an important factor which determines plastic resistivity
against the dislocation motion. The behaviour of the
indented region during the propagation of stresses which
initiate the dislocations and their motion is not understood

clearly. When an indenter is pressed on the surface
of a solid, the stresses are not simply tensile or
compressive in nature. Stresses in various directions
are set up and one should treat the resultant plastic
flow as a result of these combined stresses. It is
also observed that the fundamental mechanisms of
deformation can be either slip or twin or both or at
times facture.

(i) Slip is the most common mode of plastic
deformation, which is characterised by the displacement
of one part of the crystal relative to another along
certain definite crystallographic planes. The movement
is concentrated in a succession of planes having the
intermediate planes. The slip planes are usually of low
indices and the slip directions are those of closely
packed ones in a crystal structure.

(ii) Certain crystals may also deform by twinning,
a mechanism by means of which a portion of a crystal may
change lattice orientation with respect to the other in
a definite symmetrical fashion. Schmidt and Boas (1955)
described the twinning as the simple sliding of one plane
of atoms over the next, the extent of the movement of

each plane being proportional to its distance from
the twinning plane. Partridge (1964) studied the micro-
hardness anisotropy of magnesium and zinc single crystals.
He observed twin in above crystals and concluded that
the resolved shear stress criterion is insufficient to
account for the observed distribution of twins and any
analysis which attempts to relate deformation twinning
with hardness anisotropy must take into account the
dimensional changes which occur during twin formation.
Indenting diamond flats with diamond indenter Phaal
(1964) reported the slip and twinning of diamonds.
Vahldick et al. (1966) studied the slip systems and
twinning in molybdenum carbide single crystals with the
help of Knoop and Vickers indenter. When indented
crystal is etched by a dislocation etchant rosettes
are formed on some crystals (usually alkali halides)
indicating the dislocation distribution around an
indentation. Dislocation loops are also formed around
the indentation mark in ceasium iodide and sodium chloride
(Urusovskaya, 1965 and Kubo, 1970).

Many workers have proposed some or other
explanation for the microcrack formation during indentation
of a crystal surface. Smakula and Klein (1951) from their

punching experiments on sodium chloride explained the
crack formation on the basis of shear on slip planes.
Gilman (1958) attributed these microcracks which have
a definite crystallographic direction to the piling up
of dislocations on the slip plane. Breidt et al. (1957)
observed that crack formation is less at higher tempera-
tures (375°C) than at lower temperatures (25°C). The
cracks are usually observed to propagate from the corners
of the impression.

The interferometric studies of indented surfaces
have revealed the nature of the deformation and the
history of the sample under test. Votava et al. (1953)
were the first to study the deformed region on the
cleavage faces of mica and sodium chloride. Tolansky and
Nickols (1949 and 1952) studied the indented surfaces
of steel, tin and bismuth. They observed maximum distortion
along the medians bisecting sides of the square and minimum
along diagonals, showing thereby that no distortion
projects beyond the diagonal. They could easily show the
differences between 'piling-up' and the 'sinking-in' with
the help of FECO fringes. They established interferometrically
that the asymmetry in the fringe pattern is purely crystallo-
graphic and depends on the previous history of the samples,

and has nothing to do with the orientation of the
square of the indentation. They (1952) concluded that
the convex sides, corresponding to the extended wings
in interference pattern were 'piled-up' regions and the
concave sides were 'sink-in' regions. Satyanarayan
(1956) observed barrel or pin-cushion shape of indentation
marks interferometrically and gave idea about 'sinking-in'
which occurs mostly at faces with very little along the
diagonals of the indentation mark.

In crystalline materials plastic deformation
or slip occurs through the movement of line imperfections
called dislocations. As dislocations are multiplied (by
one of several mechanisms) during deformation, their
spacing decreases and they interact and impede each
other's motion, thus leading to work-hardening. The
strength of the dislocation interference depends on the
                                   on
nature of the crystal and the ratio of the temperature
of deformation to the melting point of the crystal.

In general, hardening of crystals can be
accomplished by the introduction of any barrier to
dislocation motion. This can occur by (a) work-hardening
(b) impurity hardening (impurities tend to segregate to

dislocations and pin them) (c) decreasing grain size
in a polycrystal (grain boundaries are barriers to
dislocation motion) (d) dispersion of fine particles
्द of second phase in the crystal and (e) phase transfor-
mations (by quenching).

It can be seen from this brief summary that
the amount of plastic deformation induced in a material
by an indenter under load depends in a complicated way
on variety of factors which defy simple analysis.

7.4   VARIATION OF HARDNESS WITH LOAD:

For geometrically similar shapes of the indent
marks for all loads, it can be shown that the hardness
is independent of load. But this is not completely true.
It is clear that during a hardness test the formation of
indentation mark leads to an increase in the effective
hardness of the material and so the hardness number
obtained is not the actual hardness of the material in
the initial state. This is mainly due to the work
hardening of the substance during the process of indentation
which will be varying with the load. Attempts have been
made to determine the absolute hardness by eliminating
work hardening. This can be done only, if the method does

not appreciably deform the substance plastically.
Absolute hardness was found to be one third of the
normal hardness by Harrise (1922).

A large number of workers have studied the
variation of hardness with load and the results given
are quite confusing. Their findings are summarized
below: Knoop et al. (1937); Bernhardt (1941) etc.
observed an increase in hardness with the decrease in
load whereas Campbell et al. (1948), Mott et al. (1952)
etc. observed a decrease in hardness with the decrease
in load. Some authors e.g. Taylor (1948), Bergsman
(1948) reported no significant change of hardness with
load.

In view of these different observations it has
become rather difficult to establish any definite
relationship of general validity between microhardness
values and the applied load. There are two ways of
studying this relationship. One is to study variation
of P with H_v directly, and other way of studying this
relationship is by plotting the graph of logP and log d.
Kick (1885) has given an empirical rule

$$P = ad^n \qquad\qquad (1)$$

Here P and d represent mean load and diameter (diagonal) of the impression respectively while 'a' and 'n' are the constants of the material under test. From the definition of Vickers hardness number

$$H_v = \frac{2 \sin 68° P}{d^2} = \text{Constant } \frac{P}{d^2} \qquad (2)$$

From the above two equations

$$H_v = a_1 d^{n-2} \qquad \text{or} \qquad H_v = a_2 P^{\frac{n-2}{n}}$$

It has been shown that in the case of Vickers microhardness the value of exponent n is equal to 2 (Kick's Law, 1885) for all indenters that give geometrically similar impressions. This implies a constant hardness value for all loads.

Hanemann and Schulz (1941) from their observations concluded that in the low load region 'n' generally has a value less than two. Onitsch (1947) found such low values of n (1 to 2.0) by observing variation of hardness with load while Grodzinski (1952) found variation of n values from 1.3 to 4.9; the value of n was nearly found to be 1.8. The standard hardness values thus obtained

were expected to yield constant results, but the actual
results obtained by different workers revealed disparities
amounting to 30-50% . Due to this variation in the results,
a low load region was selected which led to the definition
of an independent region of "microhardness". The hardness
values so obtained for this region again showed scattered
results even though the apparatus had a good mechanical
precision. The scattered observations may be attributed
to the following reasons:-

(1) Equation i.e. $P = ad^n$ is not valid.

(2) Microstructures excercise a considerable
influence on the measurements involving
very small indentations.

(3) The experimental errors due to mechanical
polishing, preparation of specimen, vibrations,
loading rate, shape of indenter, measurement
of impression, affect the hardness measurements
considerably.

The term connected with the above test, micro-
hardness means the microindentation hardness, as it
actually refers to the hardness measurement on the micro-
scopic scale. Some authors prefer the term low load
hardness for the above term. This confusion has arisen

because these ranges have not been defined sharply.
However, three possible regions of Vickers diamond
pyramid indentation testing can be defined as follows:-

(1) Microhardness: From the lowest possible
loads upto maximum of 200 gm and diameter
of indentation upto 30-50 microns. The most
characteristic region comprises of loads
from 1 to 50 gm (5 to 15 microns diagonal
length).

(2) Low load hardness: Loads from 200 gm to
3 kg and diameter of indentations upto about
300 microns. The most characteristic region
comprises of loads from 200 gm to 1 kg.

(3) Standard hardness: Loads of over 3 kg.
This test is also referred to as the micro-
hardness testing.

Since the present study is made in the region
of microhardness as defined in (1) above; the following
present a brief review of the work reported on microhardness
of various crystals.

In the recent work done by many workers (1960
onwards) the hardness has been found to be increasing at

low loads, then remaining constant for a range of
higher loads. Murphy (1969) studied hardness anisotropy
in copper crystal; variation in hardness by plastic
deformation is shown to be in part due to the escape of
primary edge dislocations.

Sugita (1963) while studying the indentation
hardness of Ge single crystal, found that occurrence of
ring cracks was suppressed relative to radial cracks
as the temperature increased and the load required to
produce the observable cracks was increased as the
temperature is raised. The temperature at which the
microscopic slip lines become observable was higher in
heavily doped crystals than in high purity crystals,
indicating that dislocation multiplication was strongly
affected by impurities.

Kosevich and Bashmakar (1960) studied the
formation of twins produced in Bi, Sb, Bi-Sb, Bi-Sn
and Bi-Pb single crystals under the action of concentrated
load by a diamond pyramid microhardness tester. They
showed that the length (l) of twins was proportional to
the diagonal (d), of the indentation and the intensity
of the twinning thus given by the coefficient α in the

equation $1 = a + \alpha d$. The value of α was more for
homogeneous alloys and was increased with Sb content
and remains constant for higher concentration of Sn
and Pb.

The variation of hardness with load was also
studied by Shah and Mathai (1969), who explained hardness
in terms of slip taking place due to deformation in the
crystal (tellurium). Edel'man (1964) showed that micro-
hardness of InSb and GaSb single crystals decreased
exponentially with temperature. The presence of deflection
points on the curves at $0.45-0.50$ T_m indicate the deformation
by slip. The activation energy for plastic flow in InSb
and GaSb was estimated 0.6 ev.

Samsonov et al. (1970) studied temperature
dependence of microhardness of titanium carbide in the
homogeneity range and found that the hardness decreased
with decrease in carbon content in carbide and also
determined the activation energies of dislocation
movement by a plastic deformation.

Hardness variation was also studied with respect
to the impurity content, dislocation density and the
change in mobility of dislocation by various workers.

Mil'vidski et al. (1965) observed decrease in hardness
with increase in concentration of impurity and dislocation
density in silicon single crystals. Kuz'memko et al.
(1963) showed decrease in the hardness due to the change
in the mobility of the dislocations as a result of
excitation of electrons during lighting and their
transition to higher energetic zone in titanium iodide
and termed this a 'photomechanical effect'. Beilin and
Vekilov (1963) observed decreased in the hardness up to
60% illumination in Ge and Si. Decrease in the hardness
was attributed to the induced photoconductivity, which
altered the widths of the dislocation cores at the sample
surface and in turn altered the plasticity.

Westbrook and Gilman (1963) studied electro-
chemical effect in a number of semiconductors. They
observed decrease in the resistance of semiconducting
crystals to mechanical indentation in the presence of a
small electric potential (0.05 to 10 v) between the
indenter and the crystal surface. This was found to be
due to significant enhancement of the surface photovoltage
by a longitudinal electric field.

The anisotropic nature of microhardness of
semiconductor was studied by Tsinzerling et al. (1969)

They observed that the anisotropy was connected with anisotropic bonding and with the position of the cleavage planes relative to the movement of the indenter.

The variation of hardness in number of semi-conductors was studied in terms of concentration of charge carrier, mobility and their interaction by many workers. Osvenskii et al. (1968) observed decreased in microhardness due to increase in carrier concentration for different contents of donor and acceptor impurities for GaAs and InSb semiconductors. In addition to this they also showed that decrease in hardness was independent of the type of carrier. Smirnov et al. (1969) studied the temperature dependence of the carrier density and mobility of Ge crystals after irradiation with electrons and during various stages of annealing. They observed that the microhardness of ⌐ such crystals did not recover fully their initial value and this was attributed to the interaction between radiation defects and dislocations, which could act as sinks or condensations for components of Frankel pairs. Seltzer (1966) who studied the influence of charged defects on mechanical properties of lead sulphide found that the rosette wing length and hardness were nearly independent of concentration of free electrons in n-type,

while had marked dependence on concentration of holes in p-type. For a hole concentration about 8×10^{-7} cm^{-3}, rapid hardening was observed with an attendant decrease in rosette size. It was suggested that this behaviour results from an e.s. interaction between charged dislocations and acceptor point defects.

Perinova and Urusovskaya (1966) studied the hardening of NaCl single crystals by X-rays and found the increased in microhardness by irradiation due to pinning of dislocations in irradiated samples and that the pinning was not destroyed by illumination. The effect of irradiation was also studied by Berzina and Berman (1964) who have a relationship between the length of the rays of the etch figure star and proton irradiation dose in LiF, NaCl and KCl single crystals.

Because of substantial effect of surface layers on the microhardness, the increase in the microhardness was observed when the applied load was reduced (Upit et al., 1969). They showed the ratio p/l^2 (where l is the length of rays in dislocation rosette around an indentation mark) was not constant (p against l^2 was not linear) at low loads due to retarding influence of the surface on the motion of dislocations. Further (1970) they estimated the change of

the mechanical properties of the crystal as the
indentation depth decreased on the basis of correlation
between the size of an indentation mark and the length
of dislocation beam.

The distribution of dislocations around an
indentation mark was studied using chemical etch pit
technique by Urusovskaya and Tyagaradzhan (1965). They
found large number of prismatic loops. They examined
the process of interaction of dislocations in crystals
having CsCl lattice. Shukla and Murthy (1968) also
studied the distribution of dislocations in NaCl single
crystals. They found increase in the distance travelled
by leading dislocation with increase in load. They
further observed the impurity had little effect on the
dimensions of the indentation but had a pronounced effect
on the length of the edge rays of the 'star pattern'
and the ratio of the mean diagonal length to the mean
length of the edge rays was nearly constant. Matkin and
Caffyn (1963) observed increase in the hardness (DHN) with
increase in Ca^{++} concentration in NaCl, while the distance
travelled by leading dislocation was observed to decrease.

The effect of impurity on hardness was also
studied by various workers. Dryden et al. (1965) studied
the hardness of alkali halides when low concentration of

divalent cations are incorporated in the crystal lattice
on the basis of dielectric measurement of doped alkali
halides crystals. They observed following effect of the
state of aggregation of the divalent impurities on the
critical resolved shear stress: (1) the increase in
critical shear stress was proportional to $C^{2/3}$, where C
is the concentration of divalent ion-vacancy pairs, (2)
there was no increase in hardness as these divalent ion-
vacancy pairs aggregate into groups of three (trimers),
(3) in $NaCl:Mn^{++}$, $KCl:Sr^{++}$ and $KCl:Ba^{++}$ there was no
increase in hardness as these trimers grow into large
aggregates, (4) in $LiF:Mg^{++}$ there was a large increase in
hardness as the trimers grow into larger aggregates and
(5) in $NaCl:Ca^{++}$ the hardness increases as a second region
of dielectric absorption appears. They have also concluded
that the structure of the trimer was same in all these
crystals and the trimer can grow in two ways, one of which
produces an increase in the resistance to movement of
dislocations. Urusovskaya et al. (1969) investigated the
influence of impurity on the strength of crystals, micro-
hardness, length of dislocation rosette rays and velocity
of dislocation movement in CsI crystals. Takeuchi and
Kitano (1971) reported the softening of NaCl crystal due
to introduction of water molecules. The plastic resistance

was almost independent of dislocation velocity except
at very high velocities. It was, however, strongly
influenced by temperature, impurities, radiation damage
and structure of the core of dislocation. Gilman (1960)
observed a sharp drop in plastic resistance of covalent
crystals at roughly about two-third of the melting
temperature and suggested that the drop was because the
cores of dislocation in covalent crystal "melt" at this
temperature. Temperature dependence of microhardness
was also studied by Sarkozi and Vannay (1971). They
concluded that besides thermal stress the observed hardening
may be due to dislocation piled-up at various impurities,
to complexes in solid solution and vacancy clusters which
were developed at high temperature and by quenching the
clusters become distributed in the crystals as fine
dispersions.

The above represents a brief review of the work
done on hardness of various crystals. The present work
is centred on the study of the variation of load with
diagonal length of indentation mark, of the variation of
hardness with load and electrical conductivity of natural
calcite crystals and synthetic potassium chloride crystals.

CHAPTER VIII

VARIATION OF LOAD WITH DIAGONAL
LENGTH OF INDENTATION MARK

CHAPTER VIII

VARIATION OF LOAD WITH DIAGONAL

LENGTH OF INDENTATION MARK

8.1   INTRODUCTION:

A variety of useful tests has been devised

wherein some kind of mechanical operation is performed

on the surface of a specimen. Quantities measured by

these surface tests are generally associated with the

term 'hardness'. Hardness as applied to amorphous and

crystalline materials has long been the subject of

discussion amongst engineers, physicists, metallurgists

and mineralogists and there are all sorts of conceptions

as to what constitutes hardness. The overwhelming

difficulty of defining hardness is that it does not

appear to be a fundamental property of material.

There is no universally accepted single test for hardness

applicable to all materials. Thus there is hardness as

measured by resistance to cutting, by scratching, by

penetration, by electrical and magnetic properties (Mott,

1956). The fundamental physics of hardness is not yet

clearly understood. The present work is taken up with

the express purpose of critically reexaming the various

formulae connected with hardness by systematically

studying 'microhardness' of natural calcite crystals.

As far as the author is aware, no such systematic work

on microhardness of cleavage faces of calcite crystal

has been made so far. In what follows the terms micro-

hardness' and 'hardness' of crystals are used to indicate

the same meaning.

8.2   EXPERIMENTAL:

Natural crystals of calcite obtained from

different localities such as Pawagarh, Chhotaudepur

(Gujarat State), Rajasthan were used for the purpose of

present study. Since the crystals from different

localities contained different types , and constrations

of impurities, small crystal cleavages from a big block

of rhombohedral calcite were used in the present
investigation. Every time freshly cleaved surfaces
were used for hardness studies. Further cleaved
crystals of approximately equal dimensions are used
so that a comparison of treated and untreated samples
can be easily made without introducing other factors.
Freshly cleaved blocks having dimensions 8 mm x 8 mm
x 2 mm were fixed on aluminium circular discs using
galva cement so that the surfaces were levelled. This
was tested by using a table microscope. Vickers
hardness tester described in Chapter II, page 26 was
used to produce indentations on the cleaved surface
by the diamond pyramidal indenter. The filar micrometer
eyepiece was used to measure the surface dimensions of
the indentation marks whereas their depths when required,
were determined by using the multiple beam interferometric
technique. To enhance the accuracy of surface measurements
the indented specimens were silvered by thermal evaporation
technique (cf. Chapter II, page 23). These silvered
indented surfaces were also used for interferometric
studies by matching them with a silvered optical flat
having appropriate reflectivity. In order to avoid the
influence of one indentation mark on the other, the
distance between two consecutive indentations was maintained

at a minimum of eight times the diagonal length of
the marks and the indentation time for all specimens
was kept 15 seconds. The load was varied from
1 to 100 gm at room temperature. Care was taken to
see that errors introduced during the work of indentation
and measurement of the dimensions of indentation mark
are avoided or minimized. The indentation marks were
produced by the diamond pyramidal indenter on the surface
in such a way that one of their diagonals always remained
parallel to a specific direction on the crystal surface.
In the case of calcite crystal, the direction [111]
represents the direction of optic axis and as such it
is a more prominent and useful direction. Its projection
on a cleavage surface of calcite is a line with direction
[110] . Hence one of the diagonals of the indentation
mark was always maintained parallel to direction [110] .

8.3   OBSERVATIONS:

The diagonal of the indentation marks produced
by various loads were measured. Several sets consisting
of a large number of observations on freshly cleaved
surfaces of calcite indented by various loads at room
temperature were taken and a typical set of observations,

TABLE 8.1

log P	log d in microns				
	303°K	473°K	573°K	673°K	773°K
0.0000	0.6021	0.6021	0.5587	0.5441	0.5740
0.3010	0.7300	0.7300	0.6990	0.6767	0.6767
0.4771	0.7782	0.7782	0.7497	0.7404	0.7404
0.6021	0.8370	0.8370	0.8129	0.7868	0.7959
0.6990	0.8960	0.8820	0.8603	0.8209	0.8370
0.7782	0.9420	0.9165	0.9031	0.8675	0.8960
0.8451	0.9777	0.9542	0.9421	0.9031	0.9165
1.0000	1.0364	1.0107	1.0261	1.0000	1.0051
1.1761	1.1303	1.1179	1.1139	1.1011	1.1139
1.3010	1.2041	1.1903	1.2041	1.1650	1.1688
1.4771	1.3065	1.2900	1.2900	1.2814	1.2639
1.6021	1.3711	1.3640	1.3711	1.3324	1.3497
1.6990	1.4150	1.4191	1.4314	1.3892	1.4043
1.7782	1.4698	1.4661	1.4624	1.4373	1.4150
1.8451	1.5282	1.5051	1.5152	1.4807	1.5217
2.0000	1.5952	1.5883	1.5740	1.5563	1.5740
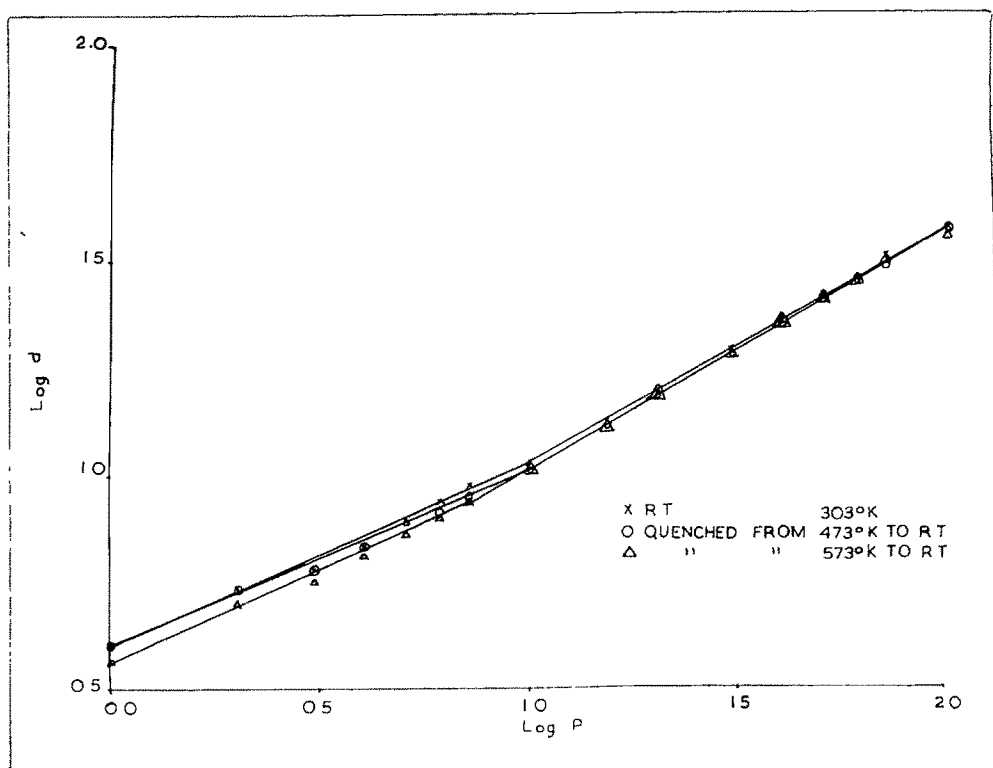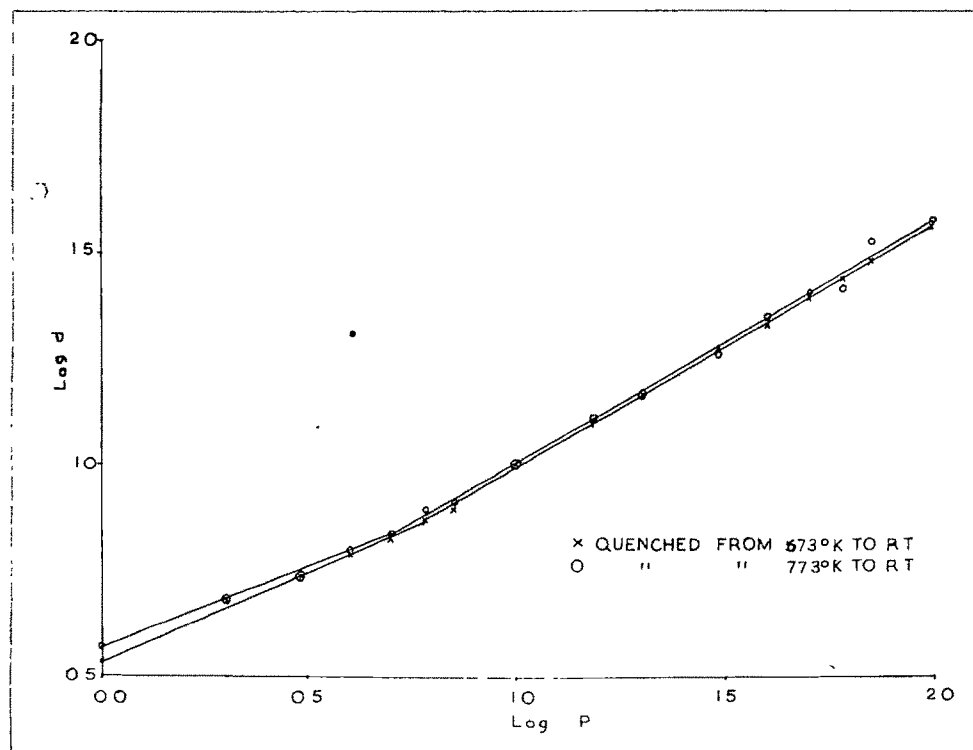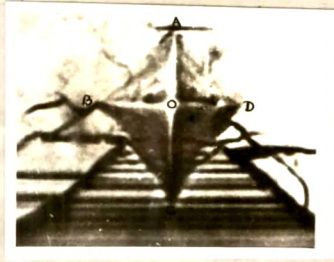
FIG.8·2

FIG.8·2

FIG.81a
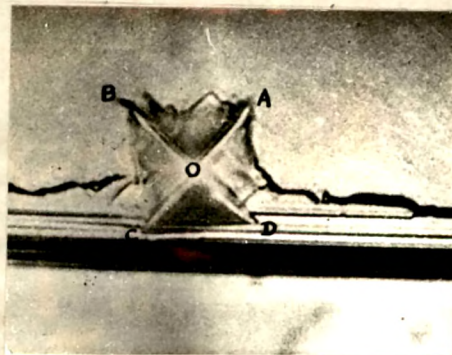
FIG.81b

recorded in Table 8.1 were studied graphically by plotting logP vs logd where P is the load in gm and d is the average value of the diagonal of indent mark in microns (Fig 8.2).

Irrespective of the applied load the impression of the indent mark on the cleaved surface is geometrically similar (Fig.8.1a) with the exception of concavity or convexity of the mark in certain cases. This curvature of sides depends upon a large number of factors (i) the nature of the crystalline material, (ii) the surface to be indented, (iii) orientation of the indenter with respect to a given direction on the surface, (iv) purity of the surface and the material, (v) the previous history of the specimen etc. However the overall shape, viz. perfect or nearly perfect square impression does not change significantly.

It is also observed that there is a noticeable change in the shape of the impression produced on an otherwise perfectly levelled specimen. This is due to several factors operating individually or simultaneously. They are as follows: (a) flatness of the surface, (b) nature and concentration of imperfections in crystals, (c) the treatment given to the surface, (d) elastic and

plastic properties of crystals, (e) crystal structure
and the arrangement of atoms on the surface of the
specimen. There is no concavity or convexity up to a
load of 50 gm while for loads of 50 gm and onwards the
concavity is observed. This curvature of the sides of
the mark is due to elastic recovery of the strained
crystal. It is observed from the orientation study
of harndess of calcite crystals (Mehta, 1972) that if
the indenter is rotated with respect to the chosen
reference direction [110] through an angle 45°, a
change in the shape of the indentation impression is
noticed (Fig 8·1b). In the present work this interesting facet
of hardness studies is not touched.

8.4   DISCUSSION AND RESULTS:

There are two ways of studying the relationship
between microhardness values and applied loads. One
way of studying this relationship was given by Hanemann
(1941) in the form of an empirical rule that was believed
to permit the intercomparison of Vickers microhardness
values. This rule states that the load 'P' is related
to the (diameter) diagonal length of an indentation mark
by the expression,

$$P = ad^n \qquad\qquad (1)$$

where 'a' and 'n' are constants of the material under
test; 'a' represents the 'standard hardness' for an
indenter of fixed diameter and 'n' giving the measure
of the variation in hardness as a function of 'P' or
'd'. The other way is to study the variation of
hardness (Vickers hardness number) directly with load.
In what follows, the detailed study on the variation
of load with average diagonal length will be presented.

The equation (1) is also known as Kick's Law.
Taking logarithms of both sides yields

$$\log P = \log a + n \log d \qquad (2)$$

The values of constants 'a' and 'n' can thus
be determined from a graph of $\log P$ vs $\log d$. Since the
relation between $\log P$ and $\log d$ is linear, the graph is
a straight line; the slope of this line gives the value
of 'n' and the intercept on the axis ($\log P$ axis) gives
the value of $\log a$ and hence 'a'. For all indenters
that give geometrically similar shapes (impressions),
Kick's law postulates a constant value of n viz. n = 2.
This implies a constant hardness value for all loads
according to the definition of Vickers hardness number(VHN).

A careful study of the graph (logP vs logd) shows that there are two clearly recognizable straight lines of different slopes meeting at a kink which is obtained at a load of about 10 gm. Further the first part of the straight line corresponding to observations taken at low loads upto load 10 gm at the kink has a slope (n_1 = 2.30) of higher value whereas for the second part of the straight line for higher loads starting from load 10 gm at kink, slope n_2 is nearly equal to 2 or less than 2. Since 'n' values are different in different regions of the graph of logP vs logd, being greater in the first region, the 'a' values also vary in the two regions, being less in the first region at low loads and more in the second one at high loads. When both the regions of the graph are considered, the kink represents a transition point or a narrow transition region which lies in the range of 5 to 10 gm. For verifying the existence of these distinguishable lines in the graph of logP vs logd, it is desirable to study the oppositely matched cleavage faces.

8.4.1 Variation of load with diagonal length of indenta-
    tion on matched cleavage faces:

It is reported in the study of etch phenomena on crystal cleavages that if a crystal is etched by an appropriate

etchant, there is perfect matching between the etch patterns observed on the oppositely matched cleavage faces. Further the multiple beam interferometric study of the topography of the oppositely matched cleavage counterparts has also convincingly proved that there is perfect matching of the topographical features on the matched cleavage faces. It is interesting to find out whether the same statement of reflection of matched features on opposite cleavage faces holds for the variation of load with diagonal length of indentation mark on the matched areas of the cleavage counterparts. With this point in mind suitable identifiable matched areas on cleavage counterparts of calcite crystals were selected and were indented in the usual way for loads raning from 1 gm to 100 gm. Graphs (not shown) of logP vs logd were then plotted. It is observed that the matching is almost perfect with almost equal values of 'n$_1$' and 'n$_2$' for both the regions of the graphs, accompanied by little deviations in 'a$_1$' and 'a$_2$' values for these regions. Since it is not possible to indent exactly matched spots on cleavage counterparts the deviations in 'a$_1$' and 'a$_2$' values are understable.

In order to verify whether the first region

in the graph is due to the deformation (cold working)

produced by the previous indentations or it is the

characteristics of the indentation load and its

penetration on the surface and the crystal, a series of

experiments were carried out on the matched cleavage

faces. The indentations were made on matched areas on

cleavage counterparts with different sets of load. Thus

a cleavage face was indented with (a) 10-100 gm load,

while its counter region on the matched face with 30-100 gm

load. Similarly indentations were made with (b) 50-100 gm

load and 70-100 gm load and (c) 1-20 gm load and 20-70 gm

load. In all the cases the graph exhibited only one line

for loads beyond the load value corresponding to kink and

that the straight line gave almost equal values of n_2

and a_2. In cases (a) and (b) the first region in the

graph corresponding to higher value of slope 'n' was missing

whereas in the first part of case (c) the first region is

observed with almost equal values of 'n_1' and 'a_1'; for

the second part of case (c) the correspondence with the

second region of the graph with normal cases (a) and (b)

reported above is excellent. These observations suggest

independent existence of first and second regions of
the graph of logP vs logd.

The study of the variation of load with diagonal
length of indentation mark on faces of different types
(c-, m-, d- and o-faces) of natural and synthetic barite
crystals (Saraf, 1971) has shown very clearly the existence
of the clearly recognisable straight lines of the graph
of logP vs logd. It is thus certain that the splitting
of the graph into two straight lines is natural and is
due to varied reactions of the crystal surfaces under
indentation.

8.4.2   Characteristics of two straight line
        regions in the graph:

The separation of the straight line graph into
two regions with different slopes indicates that in the
first region i.e. up to load of 10 gm, the value of
hardness is strictly dependent on load and in the second
region from 10 gm load onwards, this dependence on the
applied load is relatively reduced. It appears that
besides this dependence on load, there could also be other
factors contributing to this behaviour.

TABLE 8.2

Temp. in °K	n_1	n_2	$a_1 \times 10^{-2}$	$a_2 \times 10^{-1}$	Percentage change in n_1 and n_2 from std.value 2		$\dfrac{n_1}{n_2}$	$\dfrac{a_1}{a_2}$	$\dfrac{a_{1t}}{a_{1r}}$	$\dfrac{a_{2t}}{a_{2r}}$	Load at kink in gm
					$n_1\%$	$n_2\%$					
303	2.30	1.70	4.34	1.38	+15.0	−10.5	1.29	0.31	1.00	1.00	10
473	2.33	1.72	4.33	1.84	+16.5	−14.0	1.36	0.24	1.00	1.33	10
573	2.37	1.79	4.48	1.49	+18.5	−10.5	1.33	0.30	1.03	1.08	7
673	2.39	1.74	5.10	1.87	+19.5	−13.0	1.37	0.27	1.18	1.36	6
773	2.55	1.77	3.64	1.65	+27.5	−11.5	1.48	0.22	0.84	1.19	5

In order to determine the relative importance
of these factors affecting the values of 'n' and 'a' the
study was carried out on the crystal surfaces which were
thermally treated - under controlled conditions. The
specimens of almost identical dimensions were slowly
raised to a high temperature and kept at that temperature
for a few hours. They were then quenched to room tempera-
ture. The rate of quenching was kept fairly high and
was so adjusted that the crystal did not break into pieces
on quenching them from high temperature to room temperature.
The average quenching rates varied from the smallest rate
$1.6°C/sec.$, to $11.6°C/sec.$ This is indeed a slow rate
of quenching as compared to those reported in literature
for various crystalline materials. After this treatment,
the crystals were cleaved and the freshly cleaved specimens
were indented in the usual way at room temperature and a
complete set of observations were recorded and were
graphically studied. The mean values of 'n' and 'a'
obtained from several sets of observations are given in
Table 8.2. In this table are also shown the ratio of
n_1/n_2 and a_1/a_2 and the percentage changes in the values
of n_1 and n_2 from the assumed standard value 2 and also
the ratio a_{1t}/a_{1r} and a_{2t}/a_{2r} where a_{1t} and $a_2 t$ represent

the values of a_1 and a_2 at temperature $T°K$ and a_{1r}

and a_{2r} are the values of a_1 and a_2 at room temperature

(303°K). The table also records the load at the kink

point and the corresponding average diagonal length of

the indentation mark. It is obvious that the values of

'n_1' and 'a_1' for treated and untreated samples - crystal

surfaces - show comparatively large differences whereas

for the second part of the graph there are less differences

in 'n_2' and 'a_2' values for these samples (crystals). This

clearly indicates that 'n_1' and 'a_1' values are dependent

on the previous history of the specimen, whereas the

second part giving 'n_2' and 'a_2' values remains comparatively

less affected by the previous history of the specimen.

Hence the two regions correspond in general with the

structure sensitive and structure insensitive properties

of the crystal. They can roughly correspond with the

extrinsic and intrinsic properties of the crystals. Further

the initial indentation under low loads i.e. initial plastic

deformation, produces cold working of the crystal. There

will also be certain amount of recovery from this deformation.

As a result the degree of hardening of crystal surfaces

should increase. This is more true for low loads near kink.

Hence with the increase in load for indentation beyond 10 gm,

the surfaces should offer high resistance to indentation.

The hardness in this region will therefore be lower
than that in the first region, mostly near the kink. The
surface is likely to follow Kick's law and the value of
n_2 will be nearly equal to 2. In addition to the cold
working and recovery of strained crystals, several factors
such as surface energy, concentration of different types
of imperfections, interactions between like and unlike
imperfections, effect of penetration of indenter etc. are
also operating in a way unpredictable at present. The
experimentally observed deviations from the above remarks
are therefore likely to be due to these factors which are
not yet clearly understood. It is therefore difficult to
conjecture conclusively the behaviour of a crystal surface
from n_1 and a_1 values only.

8.5   CONCLUSIONS:

The following conclusions are drawn from the
above discussion:-

(i) The graph of logP against logd consists of
two clearly recognizable straight lines having
different slopes and intercepts on the axes.

(ii) The indenter load corresponding to the kink
representing a transition from one straight line
to another depends upon quenching temperature.

(iii) The slope of the first part corresponding to the
low load region of the graph is greater than that
of the second part. The intercept made by the
first line has less value than that made by the
second line.

(iv) The slopes and intercepts are temperature dependent
quantities; however, the intercepts made by the
lines are more sensitive to changes in quenching
temperatures. Out of the two intercepts (a_1 & a_2)
made by these lines, the intercept formed by the
first line corresponding to low load region is
more susceptible to quenching temperatures.

(v) The defect structures operate differently in the
low load and (comparatively) high load regions
corresponding to the two parts of the straight line.

(vi) The indentation study of the identical regions
on the oppositely matched cleavages clearly
indicate that they offer equal resistances to
various applied loads.

(vii) The splitting of the straight line into two
parts is independent of the plastic deformation
and cold working produced by low and high loads.

CHAPTER IX

VARIATION OF HARDNESS WITH LOAD

CHAPTER IX

VARIATION OF HARDNESS WITH LOAD

9.1 INTRODUCTION:

It is clear from the discussion of the previous chapter that 'standard hardness' 'a' is a function of temperature; 'a_1' and 'a_2' in general vary with temperature. However variation of a_1 with temperature is more noticeable than that of a_2. It is now interesting to study in detail how the hardness changes with temperature.

The Vickers hardness number (VHN), standardized by ASTM under the more general name Diamond pyramidal hardness (DPH) is defined by the equation,

$$\text{VHN, } H_v = 1854.4 \ P/d^2 \qquad\qquad (1)$$

where the load P is measured in gm and the diagonal
length d, of the indentation mark in microns. The hardness
number is not an ordinary constant, but a constant having
dimensions and having a deep, but less understood, physical
meaning. Combination of this equation with equation $P = ad^n$
yields

$$H_V = ad^{n-2} \quad \text{or} \quad H_V = aP^{\frac{n-2}{n}} \quad (2a, b)$$

In the case of Vickers microhardness, the value
of the exponent 'n' is equal to 2 (Kick's law, 1885) for
all indenters that gives impressions geometrically similar
to one another. Thus n = 2 implies that hardness for a
given shape of pyramid is constant and independent of load.
In order to appreciate the detailed physical meaning of
the above equations it will be instructive to consider the
example of a solid subjected to uniaxial compression. For
such a simple case, the modulus of elasticity (Young's
modulus) is given by,

$$E = \frac{\sigma}{\epsilon}$$

where σ is the compressive stress defined as load per
unit area i.e. P/A and the compressive strain ϵ is
defined as the decrease in length per unit length. Now
area of cross-section, A, increases with compression.

Hence for a constant volume of a solid, length is
inversely proportional to the area of cross-section.
If A_0 represents initial area of cross-section with
a normal length l_0, and A the final area with normal
length l after small compression, one obtains

$$lA = l_0 A_0$$

$$\frac{l}{l_0} = \frac{A_0}{A}$$

$$\therefore \; \epsilon = \frac{l - l_0}{l} = \frac{A_0 - A}{A}$$

The modulus of elasticity is therefore given by

$$E = \frac{\sigma}{\epsilon} = \frac{P}{A_0 - A} \qquad (3)$$

Hence for a simple uniaxial compressive stress
when the area is a geometrical function of the deformation,
determined here by constant volume, the resistance to
permanent deformation can be expressed simply in terms
of load and corresponding area. In indentation hardness
work the volume change is very very small. Hence the
indentation hardness can be measured by using the above
formula. Indenters are made in various geometrical shapes
such as spheres, pyramids etc. The area over which the

force due to load on indenter acts increases with the
depth of penetration. Thus the resistance to permanent
deformation or hardness can be expressed in terms of
force or load and area alone (and/or depth of penetration).
These remarks are true for solids which are amorphous
or highly homogeneous and isotropic in all directions.
In the present work, diamond pyramida indenter (DPI) is
used. Hence the discussion is specifically applicable
to the indentation work carried out by DPI.

The above analysis presents a highly simplified
picture of the process involved because there is a
great difference between deforming a solid in a simple
uniaxial compression and deforming a surface of a solid
by pressing a small indenter into it. Around the
indentation mark, the stress distribution is exceedingly
complex and the stressed material is under the influence
of multiaxial stresses. The sharp corners of a pyramidal
indenter produces a sizable amount of plastic deformation
which may reach 30% or more at the top of the indenter.
Further the surface of contact is inclined by varying
amounts to the directions of the applied force. In view
of these complications a simple expression corresponding
to that for the modulus of elasticity cannot be derived
for hardness. In the absence of any formula based on

sound theory, an arbitrary expression is used which includes both known variables - load and area - in the present case. Hence the (Vickers) hardness number, H_V is defined as the ratio of the load to the area of the impression,

$$H_V = P/A \qquad (4)$$

For pyramidal indenters the load (P) varies as the square of the diagonal, d. Thus for a given shape of pyramid,

$$P = bd^2. \qquad (5)$$

where b is a constant which depends on the material and the shape of the pyramid. The area of the impression A, is also proportional to the square of the diagonal,

$$A = cd^2 \qquad (6)$$

where c depends on the shape of the pyramid. Combination of the equations (4), (5) and (6) gives

$$H_V = \frac{bd^2}{cd^2} = b/c = \text{constant}.$$

Hence for a given shape of pyramid, hardness is independent of load and size of indentation (Kick's Law).

TABLE 5.6

P in gm	303°K			473°K			573°K		
	H_V	$\log H_V$	$\log H_V^T$	H_V	$\log H_V$	$\log H_V^T$	H_V	$\log H_V$	$\log H_V^T$
1	115.90	2.0641	4.5455	115.90	2.0641	4.7390	141.10	2.1495	4.9077
2	128.36	2.1086	4.5890	128.36	2.1086	4.7835	148.32	2.1712	4.9294
3	154.50	2.1889	4.6702	154.50	2.1889	4.8638	175.80	2.2450	5.0030
4	156.88	2.1956	4.6770	156.88	2.1956	4.8705	175.60	2.2445	5.0030
5	149.55	2.1750	4.6564	159.50	2.2028	4.8777	176.40	2.2465	5.0048
6	145.32	2.1623	4.6437	163.38	2.2133	4.8883	173.83	2.2400	4.9982
7	143.78	2.1577	4.6392	160.23	2.2046	4.8796	169.54	2.2292	4.9874
10	156.80	2.1953	4.6768	176.50	2.2467	4.9217	164.20	2.2153	4.9735
15	152.70	2.1838	4.6653	161.40	2.2079	4.8827	164.55	2.2164	4.9745
20	144.80	2.1608	4.6422	154.40	2.1886	4.8635	144.80	2.1608	4.9190
30	135.60	2.1322	4.6137	146.40	2.1656	4.8404	146.40	2.1650	4.9287
40	134.40	2.1284	4.6098	138.40	2.1412	4.8160	134.40	2.1284	4.8866
50	137.00	2.1367	4.6181	134.50	2.1287	4.8036	127.00	2.1038	4.8619
60	127.00	2.1038	4.5851	130.20	2.1145	4.7895	132.00	2.1206	4.8787
70	114.10	2.0573	4.5387	126.10	2.1007	4.7756	121.10	2.0831	4.8413
100	119.00	2.0755	4.5573	123.00	2.0899	4.7645	132.00	2.1206	4.8787

P in gm	673°K			773°K		
	H_v	$\log H_v$	$\log H_v^T$	H_v	$\log H_v$	$\log H_v^T$
1	151.40	2.1801	5.0081	131.90	2.1202	5.0086
2	164.36	2.2159	5.0426	164.36	2.2159	5.1041
3	192.54	2.2844	5.1123	183.87	2.2646	5.1529
4	197.68	2.2963	5.1242	189.84	2.2786	5.1670
5	211.30	2.3249	5.1529	196.10	2.2925	5.1780
6	204.54	2.3107	5.1386	179.46	2.2541	5.1443
7	202.79	2.3071	5.1351	190.61	2.2801	5.1682
10	185.40	2.2681	5.0962	180.90	2.2574	5.1456
15	174.60	2.2420	5.0701	164.55	2.2164	5.1045
20	173.40	2.2400	5.0671	170.40	2.2318	5.1196
30	152.10	2.1821	5.0103	164.70	2.2166	5.1048
40	160.40	2.2052	5.0334	148.00	2.1703	5.0584
50	154.50	2.1889	5.0170	144.00	2.1584	5.0531
60	148.20	2.1709	4.9989	164.40	2.2159	5.1041
70	142.10	2.1526	4.9806	117.60	2.0705	4.9586
100	143.00	2.1553	4.9834	132.00	2.1206	5.0090

In view of the defining equation (4) for hardness,
hardness number can also be considered as hardening
modulus.

Due to the complicated behaviour of indented
anisotropic single crystals of various materials and
as a result of the development of arbitrary expression
for hardness, it is clear that the theoretical treatment
of the problem is extremely difficult. Hence it is
desirable to approach this problem via experimental
observations, interpretations and with a probable develop-
ment of empirical relation(s). The present work is taken
up from this phenomenological point of view.

9.2   OBSERVATIONS:

The observations which were recorded for studying
the equation $P = ad^n$ are used for the present investigation
(Table 9.1). The Vickers hardness number, H_V is calculated
by using equation (1) for thermally treated and untreated
samples. Since the indentation work is carried out at
room temperature and a hot stage and optical components
of microscope to be used with the hot stage in a Vickers
hardness tester, are not available in this laboratory, the
quenching work is found to be more useful for studying the
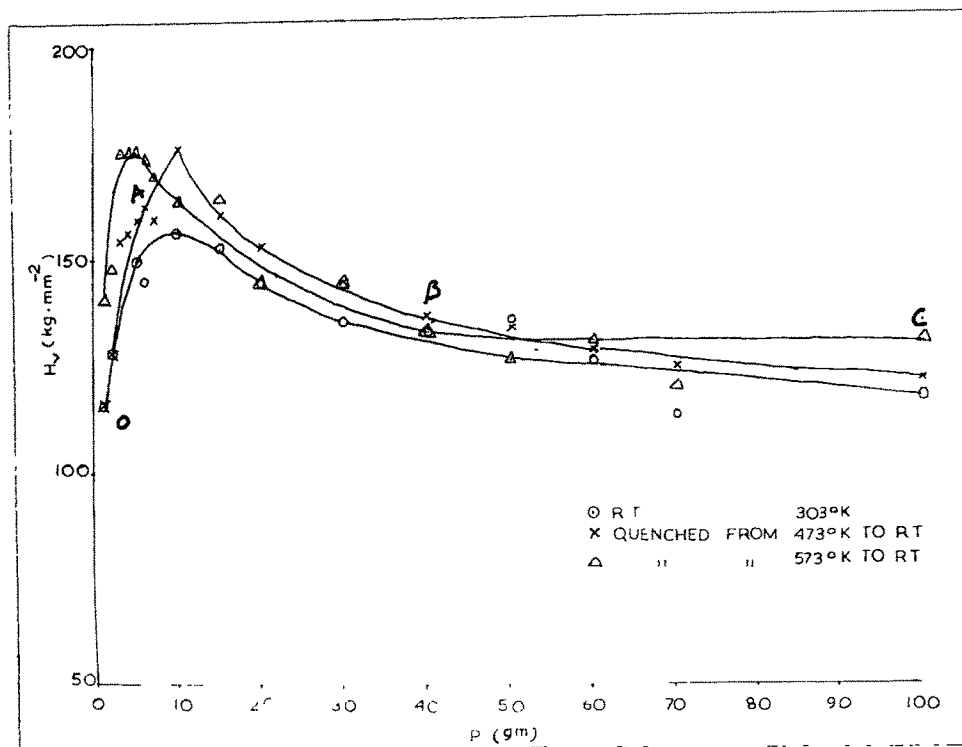
FIG.91
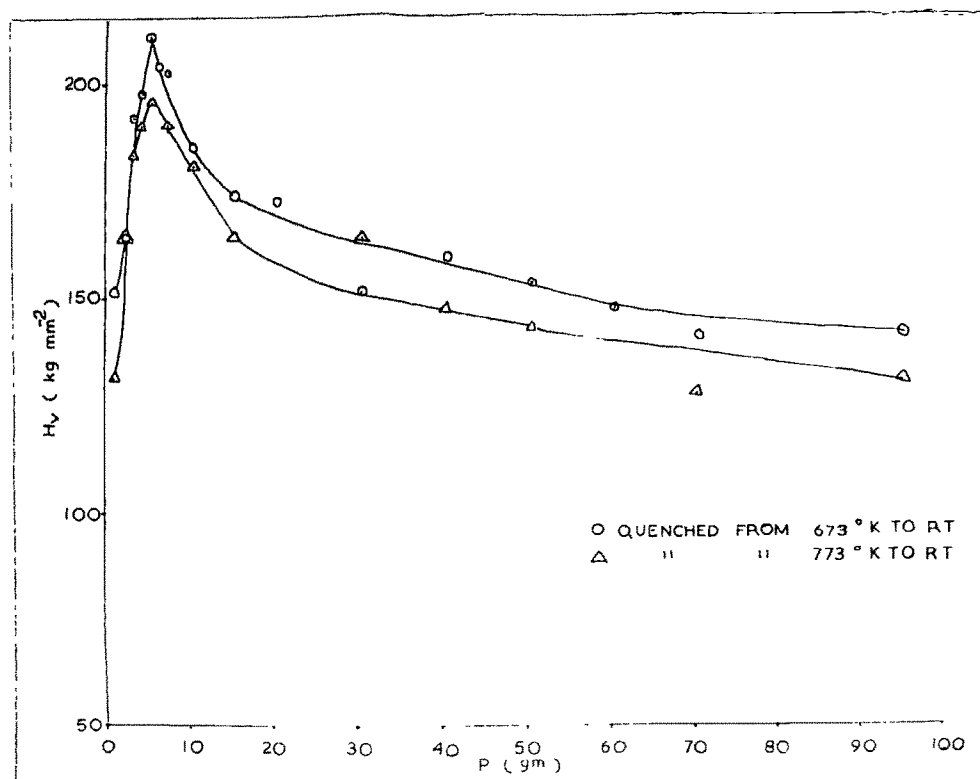
FIG.91

variation of hardness with temperature. For these
experiments, crystals of approximately equal sizes were
used. They were gradually raised to desired temperature
and kept at this temperature for identical periods
running into a few hours. They were then quenched to
room temperature. The quenching rates were so adjusted
that the quenched crystals maintained their shapes. In
the present case the rate of quenching varied from
1.6°C/sec to 11.6°C/sec. These experiments were conducted
upto a temperature of 500°C because beyond this temperature
calcite begins to decompose into CaO and CO_2 as shown by
work on thermal etching of calcite cleavages (Mehta, 1972).
Thus the conditions of the crystal kept at a constant
higher temperature are more or less maintained and hardness
value approximately corresponding to that at a constant
higher temperature is obtained by carrying out hardness
determinations at room temperature. The observations thus
obtained are graphically studied by plotting graphs of
hardness number vs load (Fig.9.1).

9.3   DISCUSSION AND RESULTS:

It is clear from the graphs that contrary to
theoretical expectations, the hardness varies with load.

The hardness at first increases with load, reaches a
maximum value then gradually decreases, and attains a
constant value for all loads. The theoretical conclusion,
thus appears to be true at higher loads only. This
behaviour is shown by all samples whether they are
thermally treated or not. The maximum value of hardness
corresponds with a load which is nearer the value of the
load at which the kink in the graph of log P vs log d is
observed. The graph of H_v vs P can be conveniently divided
into three parts OA, AB and BC where the first part
represents the highly linear relation between hardness
and load, the second part, the non-linear portion of the
graph and the third part the linear portion. It should
be noted that there is a fundamental difference between
the linear portions OA and BC of the graph OABC. This
possibly reflects varied reactions of the cleavage surface
to loads belonging to different regions. It is also
obvious from the graphs that for various higher loads,
hardness values of quenched samples are usually less than
those of thermally untreated samples, whereas for lower
loads reverse is the case. It also suggests the promi-
nence of different factors operating in these load regions.
Besides it supports to a certain extent the earlier view

about the splitting of the graph of log P vs log d into two lines.

Qualitatively the complex behaviour of micro-hardness with load can be explained on the basis of the depth of penetration of the indenter. At small loads the indenter penetrates only the surface layers, hence the effect is shown more sharply at these loads. However as the depth of impression increases, the effect of the surface layers becomes less sharp and after a certain depth of penetration, the effect of inner layers becomes more and more prominent than those of surface layers and ultimately there is practically no change in the value of hardness with load.

It is clear from the observations of hardness of quenched and unquenched samples that hardness value is effected by the thermal treatment of the specimen i.e. hardness number is a temperature dependent quantity. In order to find out the experimental mode of variation of hardness with temperature, several sets of hardness observations - determinations - were combined with temperature so that hardness could be a (i) ~~leaner~~ linear (ii) quadratic (iii) multinomial and (iv) exponential
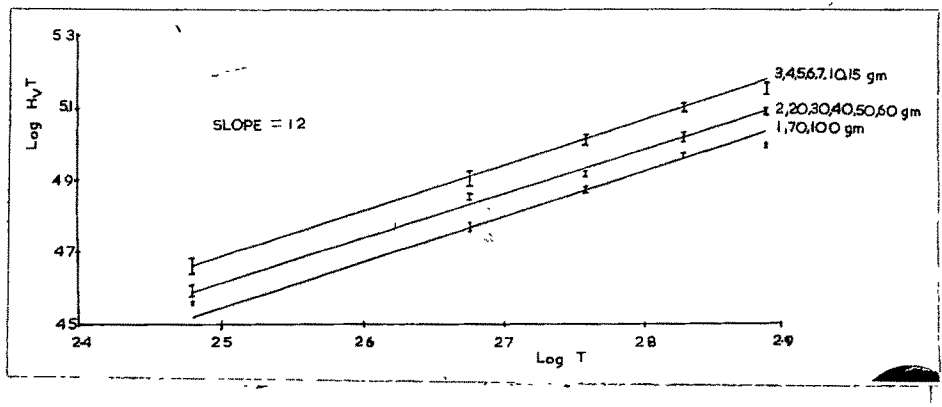
FIG.9·2
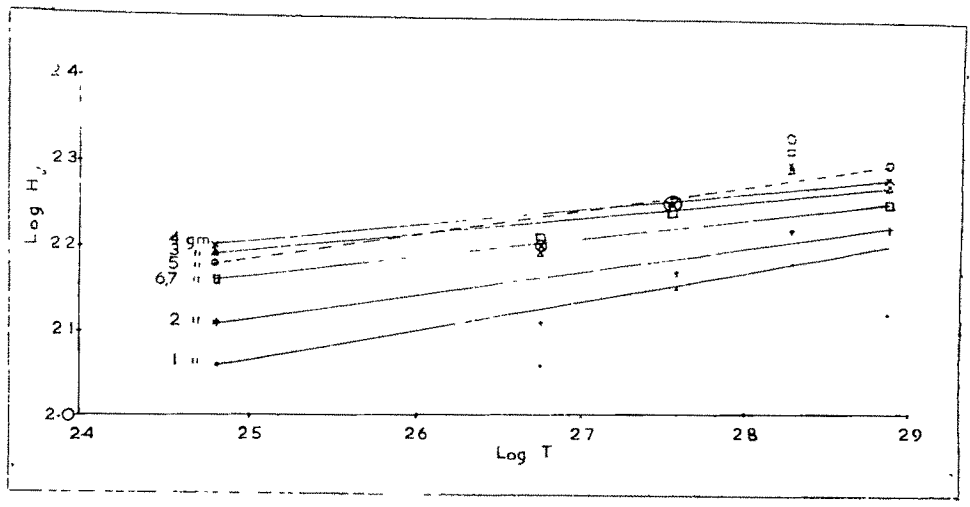
FIG.9·3

function of temperature and calculations were made to indicate the different modes of variation. In this way the quantities TH_V, H_V/T, $\log(H_V/T)$, $\log(H_V T)$ were determined. It is found that some functions show less variation in their values. Hence several graphs were then plotted by taking these functions against temperature (T), reciprocal of temperature $(1/T)$ and $\log T$. From amongst these graphs selections were made about the graphs showing a linear and highly linear characters. The graphs of $\log H_V T$ vs $\log T$ and $\log H_V$ vs $\log T$ for different loads are shown (Figs. 9.2 and 9.3). It is clear from the graphs that the variations of these functions with one another are linear. However there is one fundamental difference between these two linear characteristics. The graph of $\log H_V T$ vs $\log T$ ~~for different loads~~ are straight lines which for different loads are parallel to one another with different intercepts on axes whereas graphs of $\log H_V$ vs $\log T$ do show linearity but the intercepts made by them on the axes and their slopes are different for different loads. Hence so far as the slopes are concerned, load is apparently not associated with the variables-hardness and temperature - in the former case whereas in the later case the applied load is involved
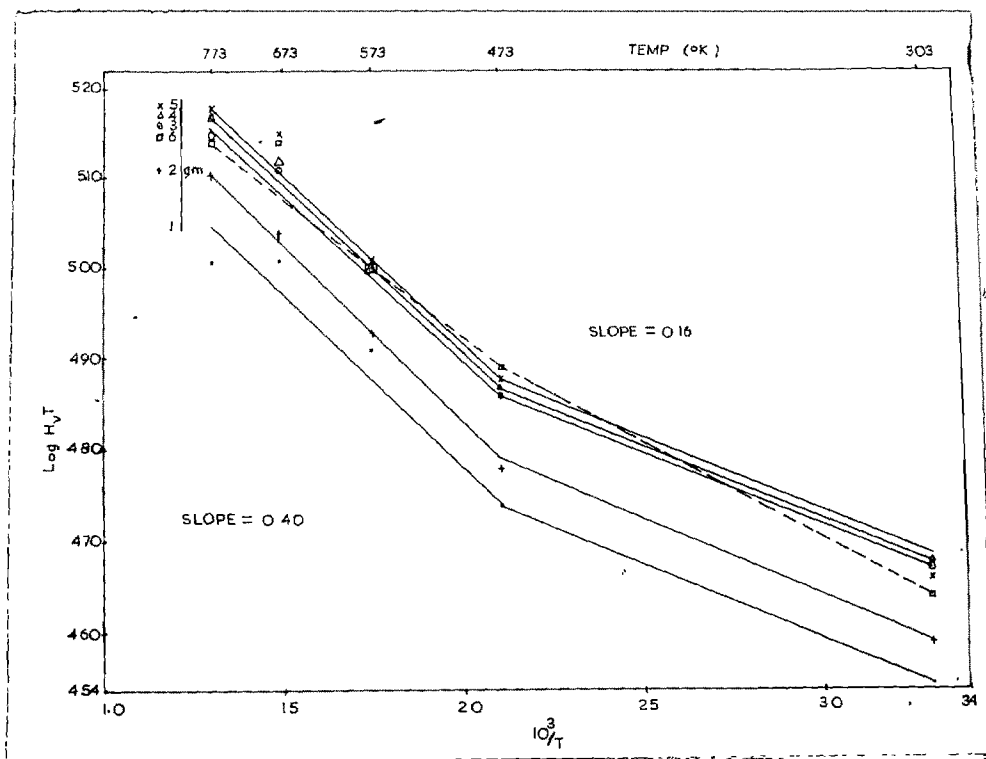
FIG.94

as one of the parameters along with hardness and temperature. Fig. 9.4 shows the plot of $\log H_v T$ vs $1/T$. Again these plots exhibit straight lines which are almost parallel to one another having identical slopes and different intercepts on the axes. All these three sets of graphs indicate that hardness is closely connected with temperature. However it is difficult to derive a definite function involving hardness, load and temperature. The slopes of these lines are given on the corresponding plots.

There are several temperature dependent crystal properties. One such property is electrical conductivity which varies in an exponential fashion with temperature. The comparison of electrical conductivity measured at a temperature T to the microhardness value of the same sample determined at the same temperature could provide a clue about the possible relation between the two quantities hardness and temperature and also between hardness and electrical conductivity of calcite crystals. Hence a study of the electrical conductivity of calcite crystals is made.

9.4   <u>CONCLUSIONS</u>:

(i) For all treated and untreated samples, the
graph between hardness and load consists
of three portions - linear, nonlinear and
linear portions.

(ii) The hardness values of quenched samples
for low loads are higher than the corres-
ponding values at room temperature; for
high loads, the reverse is the case.

(iii) The hardness is a temperature dependent
quantity.

CHAPTER X

ELECTRICAL CONDUCTIVITY OF CALCITE CRYSTALS

CHAPTER X

ELECTRICAL CONDUCTIVITY OF CALCITE CRYSTALS

10.1   INTRODUCTION:

On scanning through the literature it is found

that very less work is reported on the study of electrical

conductivity of calcite crystals.   It is therefore decided

to carry out a detailed systematic study of electrical

conductivity of the natural crystals of calcite.

10.2   EXPERIMENTAL:

Small cleaved specimens of calcite crystals were

obtained from a fairly big rhombohedral crystal of calcite.

It may be remarked here that from the same big crystal

1	FRAME	3	ELECTRODES
2	CERAMIC PLATES	4	CRYSTAL
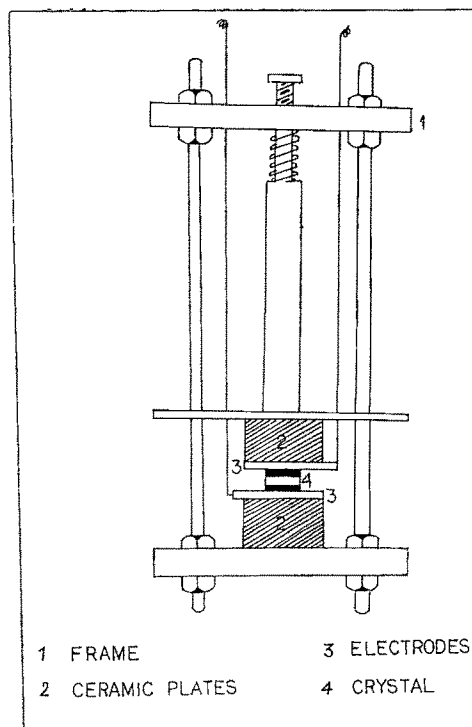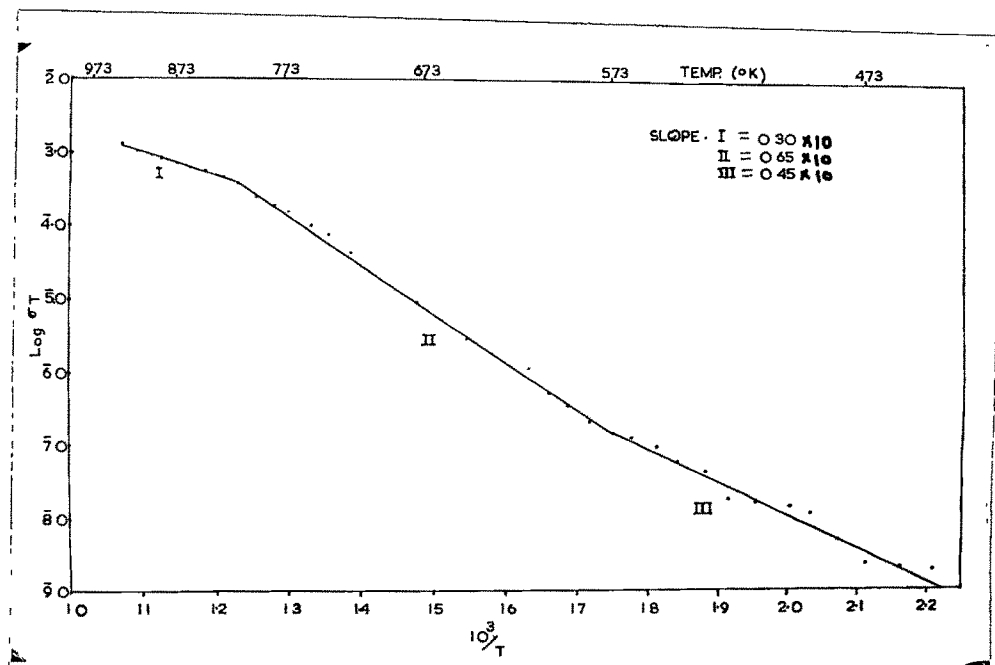
FIG. 10·1

FIG. 10·2

small cleaved specimens were used for hardness studies reported earlier. This is done with the definite intention of retaining as a common factor the same concentration of impurities of different types in natural crystals so that comparative study of hardness and conductivity could avoid their major consideration.

The dimensions, viz. length, breadth and thickness of calcite specimens used for determination of conductivity were measured by a micrometer screw and the conductivity was studied along $\langle 100 \rangle$ direction. The crystal surfaces $\{100\}$ in contact with the conducting plates of a crystal holder (Fig. 10.1) were coated with aquadag or silver films for obtaining good electrical contacts. The silvered samples could not be used for high temperatures ($\sim 200^\circ C$) because of the oxidation of silver films. Platinum foils with or without graphite paint were also used as contact electrodes. The crystal holder containing crystal in close contact with metal plates and leads was placed in a furnace designed by the author and the conductivity was determined by the impedence bridge (LCR bridge) described in Chapter II, page 33 at the ambient crystal temperature.

TABLE 10.1

T	σ	$\log \sigma T$	$10^3/T$
453	4.395×10^{-12}	$\bar{9}.2991$	2.208
463	4.923×10^{-12}	$\bar{9}.3579$	2.160
473	5.603×10^{-12}	$\bar{9}.4227$	2.114
483	5.404×10^{-11}	$\bar{9}.7327$	2.070
493	1.213×10^{-11}	$\bar{8}.0840$	2.028
503	1.547×10^{-11}	$\bar{8}.1897$	1.988
513	1.804×10^{-11}	$\bar{8}.2562$	1.949
523	2.151×10^{-11}	$\bar{8}.3326$	1.912
533	4.686×10^{-11}	$\bar{8}.6708$	1.876
543	6.668×10^{-11}	$\bar{8}.8240$	1.842
553	1.014×10^{-10}	$\bar{7}.0200$	1.808
563	1.386×10^{-10}	$\bar{7}.1417$	1.776
573	1.660×10^{-10}	$\bar{7}.2200$	1.745
583	3.787×10^{-10}	$\bar{7}.3440$	1.715
593	6.715×10^{-10}	$\bar{7}.6000$	1.886
603	9.326×10^{-10}	$\bar{7}.7500$	1.658
613	2.051×10^{-9}	$\bar{6}.0995$	1.631
633	3.152×10^{-9}	$\bar{6}.3000$	1.580
648	4.879×10^{-9}	$\bar{6}.5000$	1.540

TABLE 10.1 (contd.)

T	σ	$\log \sigma T$	$10^3/T$
663	1.408×10^{-8}	$\bar{6}.9701$	1.508
678	1.484×10^{-8}	$\bar{5}.0025$	1.475
693	3.234×10^{-8}	$\bar{5}.3505$	1.443
708	5.441×10^{-8}	$\bar{5}.5856$	1.412
723	5.984×10^{-8}	$\bar{5}.6361$	1.383
738	1.087×10^{-7}	$\bar{5}.9047$	1.355
753	1.368×10^{-7}	$\bar{4}.0128$	1.328
768	1.995×10^{-7}	$\bar{4}.1852$	1.302
783	2.601×10^{-7}	$\bar{4}.3090$	1.277
798	3.324×10^{-7}	$\bar{4}.4237$	1.253
813	4.986×10^{-7}	$\bar{4}.6079$	1.230
828	5.567×10^{-7}	$\bar{4}.6636$	1.208
843	6.469×10^{-7}	$\bar{4}.7366$	1.186
858	7.252×10^{-7}	$\bar{4}.7940$	1.166
873	8.399×10^{-7}	$\bar{4}.8652$	1.145
888	9.768×10^{-7}	$\bar{4}.9382$	1.126
903	1.041×10^{-6}	$\bar{4}.9730$	1.107
918	1.140×10^{-6}	$\bar{3}.0196$	1.089
933	1.260×10^{-6}	$\bar{3}.0702$	1.072

10.3   OBSERVATIONS, RESULTS AND DISCUSSION:

Several sets of observations were taken and
a typical set of the observations recorded in the
Table 10.1 is graphically studied by plotting a graph
(Fig.10.2) of $\log \sigma T$ vs $1/T$. The plot consists of
three straight lines with different slopes and
intercepts on the axes of $\log \sigma T$ and $1/T$.

It is clear from the general study of electrical
conductivity of ionic crystals that the activation
energies calculated for the I, II and III parts of the
graph are 0.90 ev for room temperature to 300°C, 1.3 ev
for the region 310°C to 540°C and 0.6 ev for temperatures
beyond 540°C. It is well known that calcite $(CaCO_3)$
starts decomposing at a temperature of 500°C. The rate
of the decomposition increases with temperature. The
thermal etching of calcite cleavage faces (Mehta, 1972)
has shown very clearly that it could be effected and
studied under controlled conditions only within a restricted
range of temperature viz. 520°C to 560°C. Hence the third
part of the graph indicating temperatures above 500°C
shows the effect and onset of thermal etching. As a result
of etching the slope of this line is comparatively less

than those of lines belonging to regions I and II. In
accordance with the general understanding of the behaviour
of ionic crystals the jump activation energy is 0.9 ev
while the formation energy for the Schottky defect pair
is 0.8 ev. However it is not possible to present a much
more detailed interpretation of the actual mechanisms
operating inside the calcite crystals yielding these
energy values for the following reasons:-

(1) This work is carried out on natural crystals
of calcite obtained from different localities in India;
hence the number, type and concentrations of various
impurities associated with the crystal during its growth,
their interactions among themselves and with other defects
and the precise conditions of growth are not known.

(2) Although calcite is considered to be an
ionic crystal, it is not yet definitely known to what
extent it is 'ionic'.

The work on the electrical conductivity of
calcite is a deviation from the present work on hardness.
This deviation has arisen due to apparently strange
dependence of hardness on temperature. It is also
known that point defects which exists in crystal in

thermal equilibrium, in contrast to thermodynamically unstable defects like dislocations and grain boundaries, may contribute to mechanical properties through diffusion, e.g. creep at high temperatures. Hence it is desirable to review briefly the part played by point defects in 'hardening' the crystalline materials. It is found that more direct effects on mechanical properties of point defects, e.g. an increase in the yield stress, are caused by non-equilibrium concentrations of point defects, and on formation, their aggregates. In the present case the non-equilibrium concentrations of point defects in calcite are produced by rapid cooling from high temperatures, the resulting hardening is called 'quench hardening' as distinct from radiation hardening produced by irradiation. The 'quench hardening' is simpler amongst the two . The quenching experiments introduce the following few or all effects in a crystal:-

    (i) Excess vacancies (equilibrium concentration

        of the vacancies at higher temperature).

   (ii) Possible aggregation of some vacancies.

  (iii) Annihilation of vacancies.

   (iv) Quenching strains.

(v) Pinning of vacancies at dislocations,

grain boundaries and impurities.

(vi) Effect of interstitials and their small

aggregates.

The concentration and formation energy of
excess vacancies can be studied at low temperatures
by measuring the electrical resistivity. The main
disadvantage in this procedure is the possible aggregation
or annihilation of some of the vacancies during quenching.
Implicit in this method is the correction or avoidance
of loss of vacancies together with any production of them
e.g. by quenching strains and the effect of impurity and
the formation of the more mobile vacancies. The quenching
strains are associated with the production of vacancies.
This will be clear from the following consideration.

During the quenching of specimen, the surface
is cooler than the inside and hence it is in tension while
the inside is in compression. If the stress due to thermal
gradient is large enough, the specimen will be deformed
plastically. Since the yield stress is usually lower at
higher temperature, the inside section of the material
will then undergo plastic deformation. When the quenching

is completed and the temperature is again uniform,
the plastically deformed inside material compresses
the surface layer and vice versa. The thermal stresses
thus set up are both axial and radial. Hence the
deformation of the specimen is thus complex. Usually
point defects are produced by deformation. Hence the
production of vacancies by quenching strain must be
taken into account in any assessment of the number of
vacancies quenched into a crystal. Further the mechanical
properties of a crystal are largely determined by the
number, geometrical configurations, interactions and
mobility of dislocations contained in it. The mobility
of dislocations is mainly determined by their interactions
with other defects - structural and/or otherwise. It is
this interaction which produces 'hardening'. This
production will now be reviewed briefly.

Non-conservative motion of Jogs on dislocations
and annihilation of two parallel edge dislocations of
opposite sign, one atomic plane apart, are the main
mechanisms suggested for point defect formation during
deformation by mechanical means or by quenching. The
non-conservative motion of Jogs is possible both on edge

dislocations and on screw dislocations. For deformation,

however, Jogs on screw dislocations are more important.

Jogs on a screw dislocation are geometrically short segments

of edge dislocations. The slip plane of these Jogs is not

the slip plane of the parent screw dislocation. Hence as

the screw dislocation moves, Jogs should move in a non-

conservative manner in order to move along the screw. These

fundamental mechanisms of point defect formation are well

established geometrically, but the theory cannot predict

as yet how many of a particular species of defect are

produced under certain conditions. This is a very difficult

problem because the number and behaviour of moving dislocations

are very complicated functions of the deformation temperature,

the strain rate as well as other conditions of the specimen.

A complete understanding of work hardening is required to

solve this problem. Thus quenching produces dislocations,

grain boundaries segregation of impurities as well as point

defects. It is also observed that a physical property

suitable to detect the excess vacancies is also affected

by plane and volume defects. Hence it is necessary to

separate the effect of a particular kind of defect from the

effects of others. The procedure for effecting this ~~dislocation~~ discrimination

varies in a finer way from specimen to ~~materials~~ Specimen, materials

to materials. This is not yet perfected for all types
of materials. The interstitials act in a somewhat similar
fashion as mentioned above for vacancies.

The above presents briefly the possible effects
of quenching processes on the materials. It is now
interesting to consider the effect of these processes
on crystals. It is observed that no noticeable increase
or change in hardness is found for quenched and aged
metallic crystals. This is in marked contrast to the
pronounced change in yield stress. The reason of this
apparent contradiction is found in the observed stress-
strain curve of the quenched hardened crystal i.e. the
effect of quenching hardening disappears after a moderate
                 on
                  ∧
amount of deformation. Since hardness is a measure of
the resistance to deformation, microhardness measurements
using very small loads might detect quench hardening.
However use of small loads would determine the hardness
of only the surface layers probably a few microns deep.
It may be remarked that even in the low load region,
local deformation would be severe. Since vacancies
escape to the surface during quenching, no hardening is
to be expected in the thin surface layers in order to
detect hardening. It is therefore imperative to remove

the surface layers in order to detect hardening using
small load microhardness measurements. It is from this
view that Aust et al. (1966) quenched zone-refined lead
from near 300°C into water. Hardness was measured using
a load of 1 gm; this resulted in a depth of the indentation
of about 3 μ. The specimen showed no hardening when
tested without removing the surface layers. Further
hardening was observed when surface layers of 50 μ thickness
were removed. They also found that the region near the
grain boundary showed no hardening. This is most likely
due to be the escape of vacancies to grain boundaries during
quenching.

As far as the author is aware there does not
appear to be any systematic work on ionic crystals
reported in literature on the determination of micro-
hardness of quenched ionic crystals. The present work,
therefore, represents a systematic attempt to relate
the microhardness of quenched materials with quenching
temperature. Since vacancies anneal out at the surface
during quenching, the first few layers will not exhibit
quenching effect. As calcite has perfect cleavage plane
(100) , the quenched samples were cleaved and the
hardness studies were carried out on these freshly cleaved
specimens.

The graphs of $\log H_v T$ vs $1/T$ and $\log \sigma T$ vs $1/T$ for calcite crystals have close resemblance with one another. Hence it appears that similar mechanisms are likely to operate in the crystal. Further the plots of $\log H_v T$ vs $1/T$ are parallel to one another for loads upto 5 gm. Beyond this load the parallelism is lost for the lower temperature region of the graph. Hence it can be conjectured that the point defects are mainly responsible for increased hardness of calcite crystals due to quenching. With the increase of the load dislocations which are produced on cleavage face by indentation would start interacting with the quenched-in point defects. As a result the effect of load on indenter is reflected in the lost parallelism of graphs after a load of about 5-7 gm. This effect is observed upto a load of about 12-15 gm. After that again the graphs of $\log H_v T$ vs $1/T$ become parallel to one another. It is thus clear why the graph of hardness against load is divided into three regions. In the first region which comprises hardness values for loads upto 5-7 gm (i.e. linear region OA) the quenched in point defects operate through grown and aged dislocations ignoring to a greater extent the contribution of fresh dislocations introduced by indentations

TABLE 10.2

P in gm	logTd				
	303°K	473°K	573°K	673°K	773°K
1	3.0835	3.2770	3.3168	3.3722	3.4623
2	3.2113	3.4048	3.4572	3.5048	3.5649
3	3.2589	3.4530	3.5079	3.5580	3.6286
4	3.3183	3.4983	3.5711	3.6147	3.6840
5	3.3773	3.5568	3.6184	3.6489	3.7252
6	3.4234	3.5973	3.6603	3.6955	3.7843
7	3.4593	3.6291	3.7002	3.7311	3.8046
10	3.5177	3.6855	3.7843	3.8280	3.8934
15	3.6117	3.7928	3.8721	3.9291	4.0021
20	3.6855	3.8652	3.9623	3.9930	4.0569
30	3.7879	3.9649	4.0480	4.1076	4.1523
40	3.8526	4.0390	4.1294	4.1604	4.2377
50	3.8964	4.0919	4.1895	4.2172	4.2925
60	3.9513	4.1412	4.2206	4.2653	4.3032
70	4.0079	4.1801	4.2895	4.3088	4.4099
100	4.0766	4.2632	4.3322	4.3843	4.4623
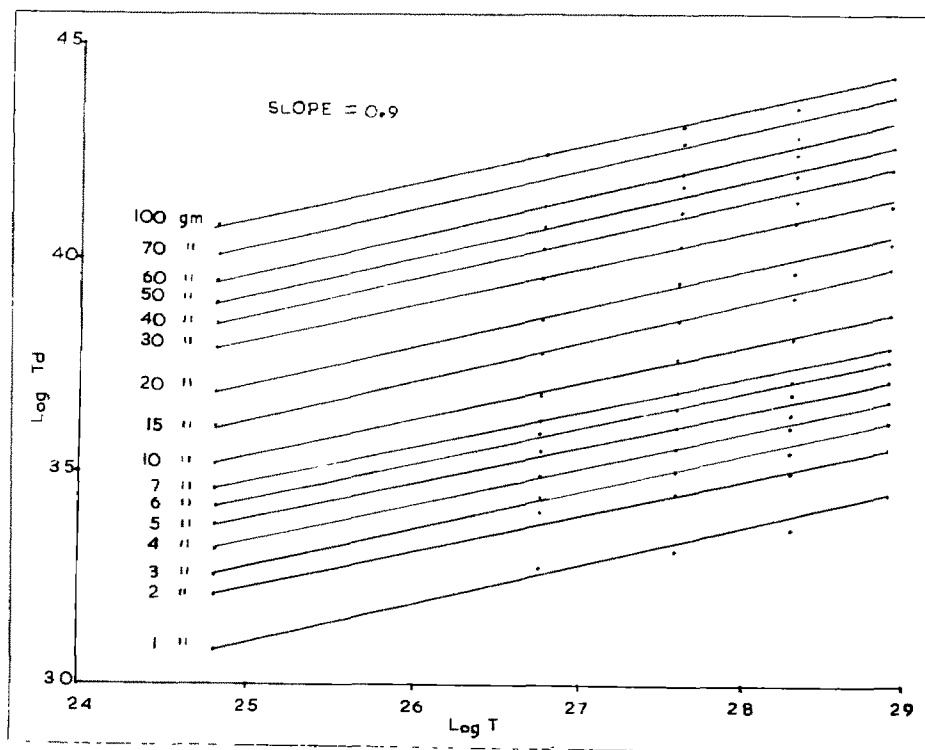
FIG.103

to hardness; at higher loads (from 12-15 gm and onwards corresponding to linear portion BC) the freshly introduced dislocations are more active than grown and aged dislocations in 'hardening' the crystals. For medium loads (associated with the region AB) there appears to be a complicated interaction between quenched-in point defects, aged dislocations and freshly introduced dislocations, resulting in the non-linear behaviour of hardness vs load. It should be remarked here that the line of demarcation between low loads and medium loads, between medium loads and high loads is not well defined.

The value of the load at which the hardness acquires a maximum value is not constant but changes with the quenching temperature. It shifts towards the lower load value. This is more clear from the graph of logP vs log d and can be inferred to a certain extent from the graphs of H_v vs P. In order to get a better picture, calculations were made for different functions involving load, average diagonal length of the impression and the quenching temperature.

It is found that the function logTd/logT has a constant value (Table 10.2) hence graphs of logTd vs logT are plotted (Fig 10.3). The interesting aspects of graphs are

the following:-

(i) They are parallel to one another for all
loads.

(ii) At a given temperature the spacing between
consecutive parallel straight lines goes on
decreasing with the increase of load.

(iii) There is no overlapping between any two lines.

(iv) All straight lines have identical slopes;
intercepts on the axes have different values
for different lines.

Calculations show that although spacing between
two consecutive lines decreases with the increase of
load, it is not zero at comparatively high loads; it
attains a minimum non-zero value. These features appear
to be connected in some way with the size and/or the
average length of diagonal of an indentation mark. This
is also shown by the shifting of the kink portion of
graphs of logP vs log d for various quenching temperatures
and the minute shifting of the peak value in the graph
of hardness against load. All these indicate the optimum
value of size or average length of diagonal of indentation
mark at which there is a transition (cf. logP vs logd graph)
or there is a decrease in hardness value from its peak

TABLE 10.3

P in gm	$\log\frac{\sigma}{H}$			
	473°K	573°K	673°K	773°K
1	$\overline{14}.6836$	$\overline{12}.3122$	$\overline{11}.9919$	$\overline{9}.1914$
2	$\overline{14}.6992$	$\overline{12}.2906$	$\overline{11}.9561$	$\overline{9}.0961$
3	$\overline{14}.5588$	$\overline{12}.2166$	$\overline{11}.8876$	$\overline{9}.0472$
4	$\overline{14}.5523$	$\overline{12}.2175$	$\overline{11}.8759$	$\overline{9}.0334$
5	$\overline{14}.5451$	$\overline{12}.2153$	$\overline{11}.8472$	$\overline{9}.0194$
6	$\overline{14}.5345$	$\overline{12}.2217$	$\overline{11}.8614$	$\overline{9}.0576$
7	$\overline{14}.5434$	$\overline{12}.2324$	$\overline{11}.8649$	$\overline{9}.0318$
10	$\overline{14}.5012$	$\overline{12}.2575$	$\overline{11}.9039$	$\overline{9}.0543$
15	$\overline{14}.5399$	$\overline{12}.2455$	$\overline{11}.9300$	$\overline{9}.0955$
20	$\overline{14}.5597$	$\overline{12}.3010$	$\overline{11}.9321$	$\overline{9}.0797$
50	$\overline{14}.6191$	$\overline{12}.3579$	$\overline{11}.9831$	$\overline{9}.1532$
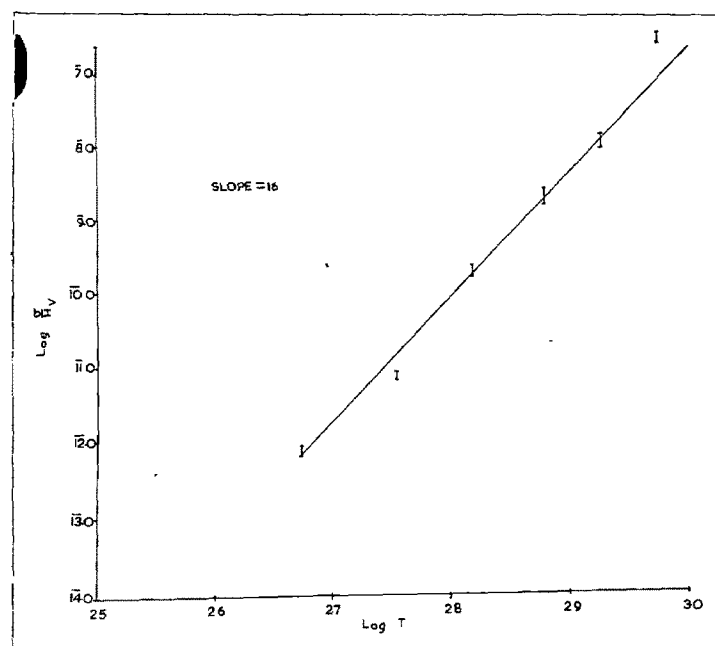
FIG. 10·4

value (cf. H_v vs P graph). For fixing up the optimum
value it is necessary to have the consideration of other
unknown factors such as the various types of treatments
given to the specimens (Saraf, 1971). Further, is the
optimum value a universal constant for all crystalline
materials? This and other questions cannot be answered
from the data available on a single crystal.

It is also clear from the above discussions
that the behaviour of hardness is similar to that of
conductivity for various quenching temperatures. Further
the low-load hardness values in the first region are
governed by the nature, distribution and concentration of
quenched-in point-defects, and their interactions with
grown and aged dislocations. Further the third region
BC of the plot of hardness vs load is governed mainly by
freshly introduced dislocations. Hence it is desirable
to discuss the comparative behaviour of these two
quantities with respect to temperature. Out of several
combinations of these quantities to form different
functions, the function $(\log\frac{\sigma}{H_v})/\log T$ has almost a constant
value (Table 10.3). Hence graphs of $\log\frac{\sigma}{H_v}$ vs $\log T$ are
plotted for different values of loads including loads of
medium range $_\wedge$ (Fig. 10.4). It is observed that there is one straight

line only which represents the variations of these

functions with each other for all loads. It is thus

clear that for a given crystal σ/H_v has a constant

value at a constant temperature for different values

of loads on an indenter. Since electrical conductivity

is proportional to the diffusion constant (Nernst-Einstein

equation) it can be concluded that for a given ionic

crystal, the ratio of diffusion constant to hardness

(number) at a constant temperature is constant for all

applied loads. This also indicates that defect structure

of the material in general and in particular equilibrium

concentration of point defects at the quenching temperature

for the same material for which two different quantities

are determined is more or less identical. However, in

view of the data available for one crystalline material,

it is not advisable to jump to this conclusion. It is

desirable to study ionic crystals of different materials

and structure, grown under controlled conditions and for

which precise data is available atleast about the variation

of one physical quantity. On going through the literature

it is observed that there are a very few papers on studies

of hardness incorporating the present view point. However

there is a large amount of literature available on the

electrical conductivity of ionic crystals. A glance
at the literature will indicate that the work on alkali
halide crystals is quite exhaustive. It is therefore
decided to take up hardness work on pure and doped
potasium chloride crystals.

10.4   CONCLUSIONS:

(1) The comparative study of hardness and electrical
conductivity of the cleavage specimens at
different temperatures indicate that the plot
between hardness and load can be qualitatively
divided into three portions, viz., low-load
region corresponding to highly linear part,
medium load region associated to non-linear
portion and high load region corresponding to
the linear portion of the graph. It is also
shown qualitatively that the (a) in the low load
region the quenched-in point defects operate
through their interactions with grown and aged
dislocations, (b) the complicated interactions
between quenched-in point defects, grown and aged
dislocations and freshly introduced dislocations
give rise to non-linear portion and (c) the
freshly introduced dislocations by indentations
at higher loads control the linear portion of the
graph.

(2) For different loads on a diamond pyramidal
indenter, the ratio of electrical conductivity
to hardness (number) of calcite crystal is
constant at constant temperature.

CHAPTER XI

MICROHARDNESS AND ELECTRICAL CONDUCTIVITY OF PURE AND DOPED POTASSIUM CHLORIDE CRYSTALS

CHAPTER XI

MICROHARDNESS AND ELECTRICAL CONDUCTIVITY OF

PURE AND DOPED POTASSIUM CHLORIDE CRYSTALS

11.1   INTRODUCTION:

The general information on potassium chloride

crystals is presented in Chapter I, and the work on

microhardness of different types of crystals in general

and of ionic crystals in particular has been reviewed

earlier (cf. Chapter VII).   The present work is taken

up with a definite intention of verifying the results

obtained from a study of the microhardness and electrical

conductivity of natural crystals of calcite reported in

the previous chapters.

11.2 EXPERIMENTAL:

A.R. quality potassium chloride (BDH) was used in the present investigation. Kyropoulos method was employed for growing single crystals of potassium chloride. The whole crystal growing unit was fabricated in the laboratory. It consists of a seed rotation arrangement alongwith the pulling arrangement. The rate of rotation and rate of pulling can be adjusted to any desired value. The furnace diameter is 7 cm, and depth 5 cm. The stabilized power (250 watts) is supplied to furnace so that its temperature can be maintained fairly constant. A fire brick of 10 cm height is used as a base for platinum crucible of 20 ml capacity used to hold the melt. When the temperature of the melt is 100°C to 200°C above the melting point, the KCl-seed (2cm x 0.5 cm x 0.5 cm) is lowered in the melt. A few outermost layers of the seed were lost due to contact with the fused mass; the temperature of the furnace is then decreased so that it is just a few degrees above the melting point. In order to keep the crystal diameter same the temperature was slowly decreased with the advancement of growth fronts. The rate of pulling was 4 mm/hour and the seed was rotated at the same rate (4 rev./hour). The pulling unit has been

designed and used to allow the seed crystal and/or melt to be rotated as the crystal is pulled. The advantages of this method over the conventional vertical pulling with zero relative speed between the melt and the growing crystal are as under:- (i) melt is effectively stirred, (ii) spurious crystal nuclei formed or being formed on the melt surface are ejected centrifugally, (iii) pulling is without any obstruction or jerks and (iv) radial temperature gradient is eliminated. This method was also used for growing doped crystals. A definite amount of dopant (A.R. quality (BDH) $SrCl_2$) by weight was mixed with a known amount of potassium chloride. The temperature of the furnace containing a platinum crucible with the (solid) mixture was then gradually raised and maintained, to a desired temperature. The crystals were then grown in the usual way as mentioned above. The grown cylindrical ingots of single crystals of 'pure' KCl and KCl:Sr were cut along the cleavage directions [100] and rectangular plates with dimensions 2cm x 1 cm x 1 cm were prepared. The crystals were transferred to an annealing furnace with a vertical temperature gradient. The temperature of the furnace was maintained constant with variation of $\pm 10°C$ by feeding a highly stabilized power supply to the furnace. The

TABLE 11.1

| log P in gm | KCl log d in microns | | | | | | | KCl:Sr^{++} 6.1x10^{-3} m.f. | KCl:Sr^{++} 19 x 10^{-3} m.f. |
	303°K	473°K	573°K	673°K	773°K	873°K	973°K	303°K	303°K
0.0000	1.1931	1.2041	1.2144	1.2430	1.2492	1.2207	1.2041	1.3171	1.1383
0.3010	1.3198	1.3222	1.3198	1.3570	1.3570	1.3273	1.3292	1.3824	1.2582
0.4771	1.3870	1.3870	1.3979	1.4254	1.4191	1.3979	1.3979	1.4510	1.3424
0.6021	1.4354	1.4492	1.4587	1.4735	1.4643	1.4492	1.4524	1.4789	1.3779
0.6990	1.4790	1.4825	1.4861	1.5152	1.5035	1.4860	1.4949	1.5051	1.4273
0.7782	1.5136	1.5202	1.5250	1.5458	1.5363	1.5250	1.5315	1.5170	1.4624
0.8451	1.5488	1.5549	1.5593	1.5784	1.5685	1.5579	1.5623	1.5426	1.5034
1.0000	1.6309	1.6360	1.6410	1.6472	1.6385	1.6360	1.6348	1.6047	1.5711
1.0414	1.6556	1.6593	1.6628	1.6651	1.6593	1.6569	1.6569	1.6140	1.5911
1.0792	1.6733	1.6824	1.6846	1.6824	1.6825	1.6767	1.6767	1.6360	1.6087
1.1761	1.7263	1.7305	1.7344	1.7284	1.7243	1.7284	1.7284	1.6868	1.6484
1.3010	1.7915	1.7924	1.7950	1.7959	1.7941	1.7941	1.7941	1.7503	1.7222
1.3979	1.8411	1.8420	1.8443	1.8451	1.8435	1.8427	1.8427	1.7993	1.7709
1.4771	1.8823	1.8823	1.8837	1.8816	1.8837	1.8829	1.8829	1.8396	1.8112
1.6021	1.9457	1.9469	1.9469	1.9494	1.9475	1.9475	1.9475	1.9031	1.8794
1.6990	1.9945	1.9945	1.9945	1.9972	1.9956	1.9945	1.9915	1.9512	1.9426

pyrometer with Rh-Pt thermocouple indicated the furnace
temperature. Its temperature was slowly and gradually
raised at a rate of 20°C/hour upto 700°C. The crystals
were kept at this temperature for 24 hours for annealing.
The furnace temperature was then lowered at the same rate.
After ensuring that all parts of furnace were at room
temperature, the crystals were taken out for detailed
study of microhardness and electrical conductivity.

11.3   OBSERVATIONS, RESULTS AND DISCUSSION:

The present study is carried out on the cleavage
faces of pure and doped potassium chloride crystals and
is divided into three parts, viz.,

(1) Variation of load with (average) diagonal
length of indentation mark.

(2) Variation of microhardness with load, and

(3) Electrical conductivity.

These parts are presented separately in the following
sections.

11.3.1 Variation of load with (average) diagonal
length of indentation impression:

The observations (Table 11.1) are taken on
freshly cleaved surfaces of thermally treated and untreated
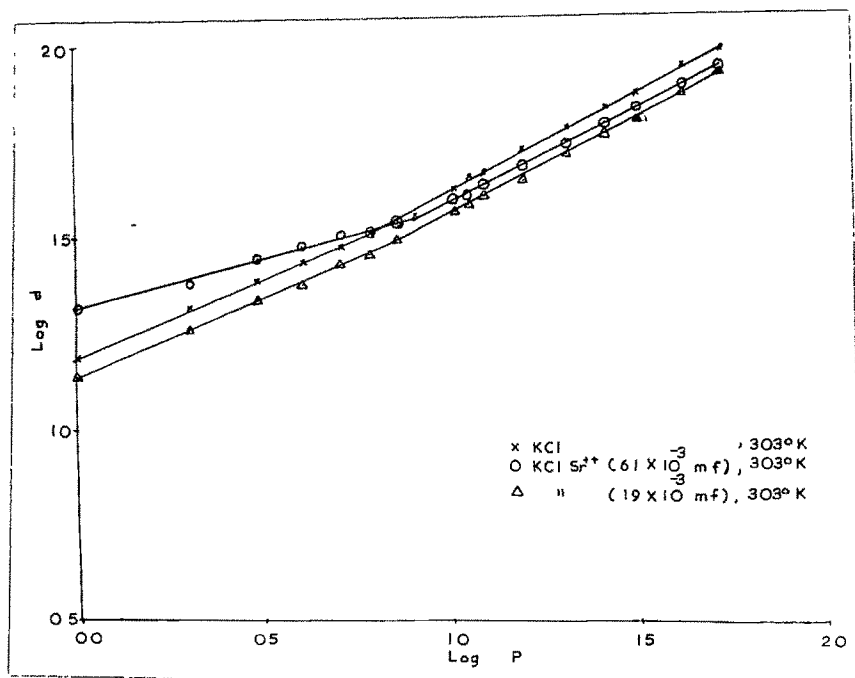
FIG.11-1
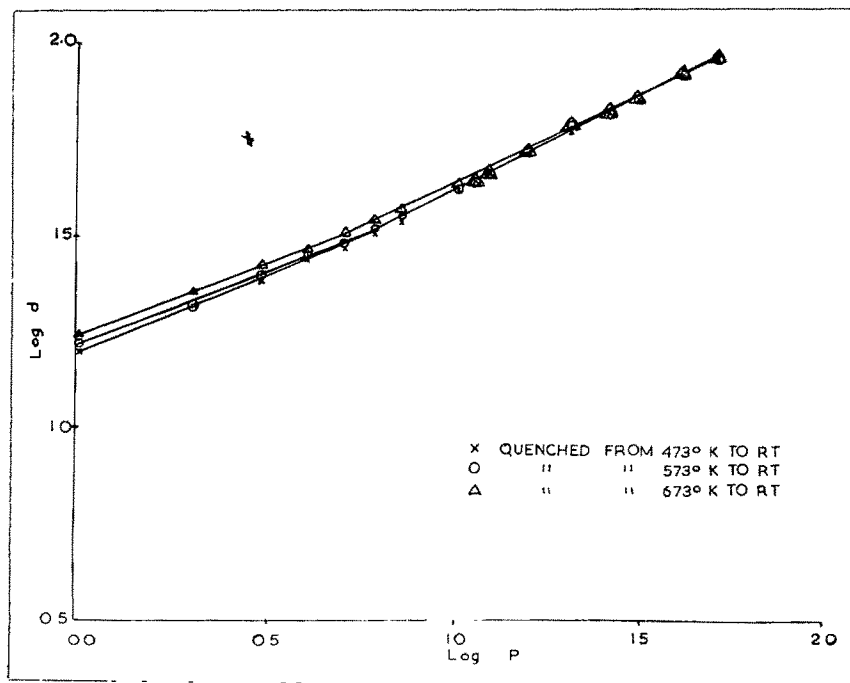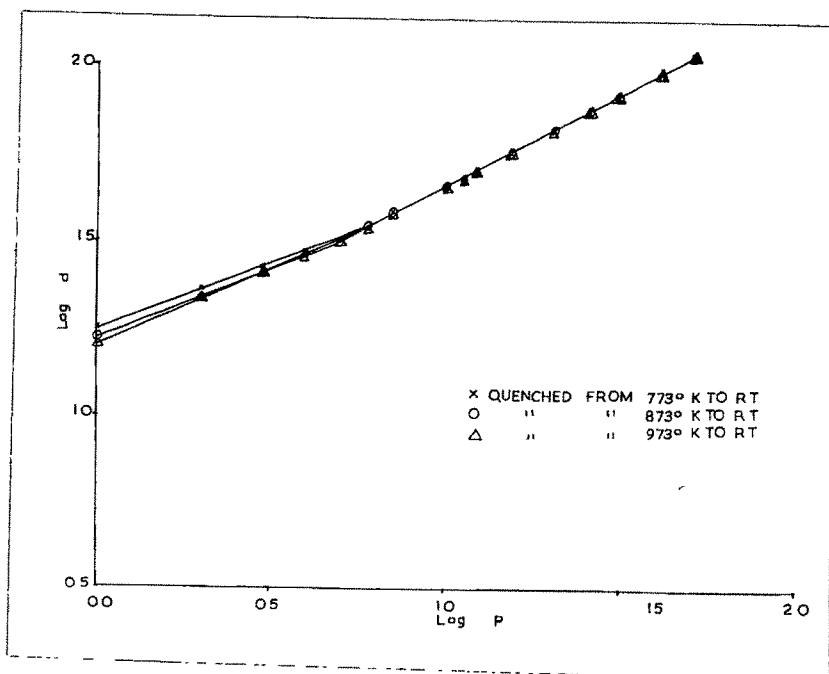
FIG. 11·1

FIG. 11·1

potassium chloride crystals by indenting them in the
usual way by Vickers hardness tester. They are graphically
recorded by plotting logd vs logP (~~Table~~ *fig.* 11.1). From the
discussion on the study of variation of load with average
diagonal length of indentation mark on cleavage faces of
calcite and a careful study of the present plots, the
following conclusions are obvious:-

(i) The (straight line) graph is split up into
two distinguishable straight lines having
different slopes and intercepts on the axes.

(ii) The load on indenter corresponding to the
kink representing a transition from one
straight line to another depends upon quenching
temperature.

(iii) The slope of the first part corresponding to
the low load region of the graph is greater
than that of the second part. The intercept
(a_1) made by the first line has less value
than that (a_2) made by the second line.

(iv) The slopes and intercepts are temperature
dependent quantities; however the intercepts
made by the lines are more sensitive to
changes in quenching temperature. Out of

the two intercepts made by these lines,

the intercept formed by the first line

corresponding to low load region is more

susceptible to quenching temperature.

(v) The defect structures operate differently

in the low load and comparatively high load

regions corresponding to the two parts of

the straight line.

(vi) The splitting of the straight line into

two parts is independent of the plastic

deformation and cold working produced by

low and high loads.

(vii) The indentation study of identical regions

on oppositely matched cleavage faces clearly

indicate that they offer equal resistances

to various applied loads.

The conclusions (vi) and (vii) were obtained by

carrying out the studies on the cleavage faces of

potassium chloride crystals in a way similar to the one

described in Chapter VIII (pages 148 and 146). In addition

to the above conclusions, a careful study of Tables 8.2

(cf. Chapter VIII, reproduced here for quick comparison)

TABLE 11.2

KC1

Temp. in °K	n_1	n_2	$a_1 \times 10^{-4}$	$a_2 \times 10^{-3}$	Percentage change in n_1 and n_2 from std. value 2		$\frac{n_1}{n_2}$	$\frac{a_1}{a_2}$	$\frac{a_{1t}}{a_{1r}}$	$\frac{a_{2t}}{a_{2r}}$	Load at kink in gm
					$n_1\%$	$n_2\%$					
303	2.36	1.93	15.99	7.06	+36.0	−7.0	1.22	0.23	1.00	1.00	6
473	2.33	2.00	17.66	5.22	+33.0	0.0	1.17	0.34	1.10	0.74	6
573	2.44	2.00	11.59	4.98	+44.0	0.0	1.22	0.23	0.73	0.71	5
673	2.59	2.06	7.84	3.87	+59.0	+6.0	1.26	0.20	0.49	0.55	5
773	2.70	2.00	4.30	5.22	+70.0	0.0	1.35	0.08	0.27	0.74	6
873	2.47	2.00	10.24	5.22	+47.0	0.0	1.23	0.20	0.64	0.74	5
973	2.40	2.00	13.24	5.22	+40.0	0.0	1.20	0.25	0.83	0.74	6
KC1:Sr(6.1x10⁻³ m.f.)											
303	3.75	2.00	0.11	6.31	+175.0	0.0	1.88	0.002	1.00	1.00	8
KC1:Sr(19x10⁻³ m.f.)											
303	2.39	1.92	18.97	9.59	+39.0	−8.0	1.25	0.20	1.00	1.00	7

TABLE 8.2

Temp. in °K	n_1	n_2	$a_1 \times 10^{-2}$	$a_2 \times 10^{-1}$	Percentage change in n_1 and n_2 from std.value 2 $n_1\%$	$n_2\%$	$\dfrac{n_1}{n_2}$	$\dfrac{a_1}{a_2}$	$\dfrac{a_{1t}}{a_{1r}}$	$\dfrac{a_{2t}}{a_{2r}}$	Load at kink in gm
303	2.30	1.70	4.34	1.38	+15.0	-10.5	1.29	0.31	1.00	1.00	10
473	2.33	1.72	4.33	1.84	+16.5	-14.0	1.36	0.24	1.00	1.33	10
573	2.37	1.79	4.48	1.49	+18.5	-10.5	1.33	0.30	1.03	1.08	7
673	2.39	1.74	5.10	1.87	+19.5	-13.0	1.37	0.27	1.18	1.36	6
773	2.55	1.77	3.64	1.65	+27.5	-11.5	1.48	0.22	0.84	1.19	5

and 11.2 reveals the following fine differences:-

(a)   The slope of the second region in case of KCl

crystals has comparatively a larger value than

the one obtained for calcite crystals. Further

its value at all temperatures except at room

temperature is exactly two - the theoretical

value reported earlier (cf. Chapter VIII, page

145). Even the room temperature value is not

much different from the 'standard' value 2.

(b)   The percentage changes in 'n_1' values from

'standard' value 2 are more noticeable in the

case of KCl crystals than those for calcite

crystals. However, for each crystal the

ratio (n_1/n_2) does not exhibit much variation.

For calcite crystals 'n_1' values increase with

the quenching temperature; such is not the case

for KCl crystals.

(c)   When the ratios of the intercepts made by two

straight lines on the axis of logP for treated

and untreated samples are considered, it is found

that although variations in these ratios are quite

small, they do not show any regularity. This is

also true for ratios (a_{1t}/a_{1r}) and (a_{2t}/a_{2r})
obtained for both crystals. Due to irregular
variations of a_1 and a_2 in both cases for
equal changes of, and values of, quenching
temperatures it is difficult to draw any
meaningful conclusion except for the fact that
they depend on temperature. As far as the
absolute values of 'a_1' and 'a_2' for both crystals
are concerned, it is found that these values for
KCl crystals are lower by a factor of 100 than
those for calcite crystals.

(d) In the case of calcite crystals the variation
in the load at kink for specimens quenched from
different temperatures is from 5 to 10 gm whereas
for the same quenching temperatures, there is
not much variation for pure and doped KCl crystals.

(e) For KCl crystals containing strantium ions, the
slope of the first part of the straight line graph
corresponding to low load region shows a significant
increase over that mentioned for relatively very
'pure' samples of KCl and the corresponding intercept
has a lower value. However with increased amount
of dopant, the slope decreases and the intercept

increases. For the straight line graph

corresponding to high load region concentration

of the dopant affects slope values to a certain

extent. For low concentration the slope value

is not at all affected. `This is not the case

at higher concentration. Further the introduction

of dopant into the host crystal (KCl) under

controlled conditions affect the values of load

at kink.

It may be remarked in passing that several workers

have reported visible scattering in 'n' values (e.g. see

Hanemann and Schultz (1941), Onitsch (1947), Grodzinski

(1952)). However, none has emphasized on the splitting

of the graph into two straight lines and on its characteri-

stics.

The fine differences observed in the behaviour

of indented specimens – pure and doped – indicate that

there are a number of factors which could be responsible

for the reactions of these treated specimens. The factors

are as follows:- (i) size of a specimen receiving the

treatment, (ii) time during which the specimen is subjected

to this treatment, (iii) constancy of quenching temperature,

(iv) structure of samples (crystals), (v) inherent impurity

in materials, (vi) non-uniform radial and axial concentra-
tion of added impurities in doped crystal. It is desirable
to discuss the possible contributions of these factors one
by one:-

The first three factors viz., size of the specimen,
time during which the specimen is given heat treatment
(i.e. time required to raise it to a desired high temperature,
time spent in maintaining it at this temperature and the
time during which quenching is completed) and maintenance
of constant temperature from which it is quenched, are
scrupulously kept common for calcite and KCl crystals; hence
for comparative study of these crystals they could be
ignored in the discussion. It is known that crystal structures
influence hardness properties of materials (e.g. graphite
and diamond). The structures of these crystals are therefore
likely to affect their hardness behaviour. KCl has a face
centred cubic structure whereas calcite has a rhombohedral
structure. However a rhombohedral structure can be produced
by introducing a desired amount of deformation of a f.c.c.
structure along a diagonal. K^+ and Cl^- ions in KCl structure
are replaced by Ca^{++} and CO^{--} ions respectively; CO_3 radical
is not having a completely planar structure. These
differences would partially or completely affect their
hardness values. However, the present study is unable to

throw light on hardness behaviour of these crystals
on the basis of their structures.

'Chemical purity' of a substance is an ideal
concept. Every chemical contains a certain amount of
impurities. This is more so for mineral crystals which
are grown under unknown conditions. No reliable
information about the amount, nature and distribution
of impurities in natural crystals of calcite is available.
Strantium chloride ($SrCl_2$) and strantium are heavier than
potassium chloride and potassium. Hence a highly uniform
homogeneous mixture of molten mass could not be prepared.
This was detected in the grown crystal. Hence during
annealing partially successful attempts were made to have
uniform distribution of dopant in KCl. Due to limited
facilities available in the laboratory the actual amount
of impurity present in studied samples (crystals) could
not be determined. Hence the dopant amount mentioned in
the graph simply indicates the maximum amount in the
grown crystal; the actual amount is bound to be less.
It is clear from the graph (fig. 11.1) that its splitting
into two straight lines is more prominent at lower concen-
tration than at higher concentration of dopant.

TABLE 11.3

KCl

P in gm	303°K H_v	$\log H_v$	$\log H_v^T$	473°K H_v	$\log H_v$	$\log H_v^T$	573°K H_v	$\log H_v$	$\log H_v^T$	673°K H_v	$\log H_v$	$\log H_v^T$
1	7.59	0.8802	3.3616	7.24	0.8597	3.5346	6.91	0.8395	3.5977	6.05	0.7818	3.6098
2	8.50	0.9294	3.4108	8.40	0.9243	3.5992	8.50	0.9294	3.6876	7.16	0.8549	3.6829
3	9.36	0.9713	3.4527	9.36	0.9713	3.6462	8.91	0.9499	3.7081	7.86	0.8954	3.7234
4	10.02	1.0008	3.4822	9.36	0.9713	3.6462	8.96	0.9523	3.7105	8.36	0.9222	3.7502
5	10.20	1.0086	3.4900	10.05	1.0021	3.6770	9.86	0.9939	3.7521	8.65	0.9370	3.7650
6	10.44	1.0187	3.5001	10.14	1.0060	3.6809	9.90	0.9956	3.7538	8.90	0.9494	3.7764
7	10.36	1.0153	3.4967	10.08	1.0033	3.6782	9.87	0.9943	3.7525	9.04	0.9562	3.7842
10	10.10	1.0043	3.4857	9.90	0.9956	3.6705	9.70	0.9868	3.7450	9.40	0.9731	3.8011
11	10.02	1.0008	3.4823	9.79	0.9908	3.6656	9.62	0.9832	3.7414	9.50	0.9777	3.8057
12	9.96	0.9983	3.4797	9.60	0.9823	3.6572	9.54	0.9795	3.7377	9.50	0.9823	3.8058
15	9.80	0.9912	3.4305	9.62	0.9832	3.6580	9.53	0.9791	3.7272	9.60	0.9872	3.8152
20	9.70	0.9868	3.4682	9.64	0.9841	3.6589	9.51	0.9782	3.7363	9.71	0.9773	3.8052
25	9.63	0.9863	3.4651	9.55	0.9800	3.6549	9.50	0.9777	3.7358	9.49	0.9777	3.8053
30	9.55	0.9800	3.4615	9.53	0.9791	3.6540	9.50	0.9777	3.7358	9.50	0.9777	3.8058
40	9.50	0.9777	3.4591	9.50	0.9771	3.6525	9.50	0.9777	3.7358	9.50	0.9777	3.8058
50	9.50	0.9777	3.4591	9.50	0.9777	3.6525	9.50	0.9777	3.7358	9.50	0.9777	3.8058

TABLE 11.3 (contd.)

KCl

P in gm	773°K H_v	$\log H_v$	$\log H_v^T$	873°K H_v	$\log H_v$	$\log H_v^T$	973°K H_v	$\log H_v$	$\log H_v^T$
1	5.88	0.7694	3.6576	6.70	0.8261	3.7671	7.24	0.8597	3.8478
2	7.16	0.8549	3.7431	8.20	0.9138	3.8548	8.12	0.9096	3.8977
3	8.07	0.9069	3.7951	8.91	0.9499	3.8909	8.88	0.9484	3.9365
4	8.76	0.9425	3.8307	9.36	0.9713	3.9123	9.20	0.9638	3.9519
5	9.10	0.9590	3.8472	9.68	0.9859	3.9269	9.50	0.9777	3.9658
6	9.44	0.9750	3.8632	9.90	0.9956	3.9366	9.60	0.9823	3.9704
7	9.60	0.9823	3.8705	9.96	0.9983	3.9393	9.73	0.9881	3.9762
10	9.80	0.9912	3.8794	9.90	0.9956	3.9366	10.00	1.0000	3.9881
11	9.79	0.9908	3.8789	9.86	0.9939	3.9349	9.90	0.9956	3.9837
12	9.60	0.9823	3.8705	9.84	0.9930	3.9340	9.82	0.9921	3.9802
15	9.58	0.9814	3.8695	9.70	0.9868	3.9278	9.72	0.9868	3.9749
20	9.54	0.9795	3.8677	9.58	0.9814	3.9224	9.58	0.9814	3.9694
25	9.52	0.9786	3.8668	9.55	0.9800	3.9210	9.55	0.9800	3.9681
30	9.50	0.9777	3.8659	9.53	0.9791	3.9201	9.53	0.9791	3.9672
40	9.50	0.9777	3.8659	9.50	0.9777	3.9188	9.50	0.9777	3.9658
50	9.50	0.9777	3.8659	9.50	0.9777	3.9188	9.50	0.9777	3.9658

TABLE 11.3 (contd.)

p in gm	KCl:Sr^{++} 6.1x10^{-3} m.f. 303°K			KCl:Sr^{++} 19x10^{-3} m.f. 303°K		
	H_V	log H_V	log H_V^T	H_V	log H_V	log H_V^T
1	4.31	0.6345	3.1159	9.63	0.9836	3.4651
2	6.36	0.8035	3.2868	11.28	1.0522	3.5338
3	9.28	0.9680	3.4490	11.61	1.0649	3.5463
4	7.84	0.8943	3.3758	13.00	1.1139	3.5954
5	9.05	0.9566	3.4381	13.30	1.1230	3.6053
6	10.26	1.0112	3.4926	13.44	1.1284	3.6096
7	10.64	1.0279	3.5084	12.74	1.1052	3.5866
10	11.15	1.0472	3.5286	13.40	1.1271	3.6085
11	12.10	1.0828	3.5642	13.53	1.1313	3.6128
12	11.88	1.0749	3.5563	13.49	1.1301	3.6115
15	11.76	1.0704	3.5518	13.34	1.1353	3.6466
20	11.72	1.0689	3.5503	13.32	1.1246	3.6059
25	11.68	1.0675	3.5489	13.31	1.1241	3.6056
30	11.64	1.0660	3.5474	13.26	1.1226	3.6040
40	11.59	1.0640	3.5455	12.92	1.1113	3.5927
50	11.98	1.0788	3.5599	12.07	1.0817	3.5621
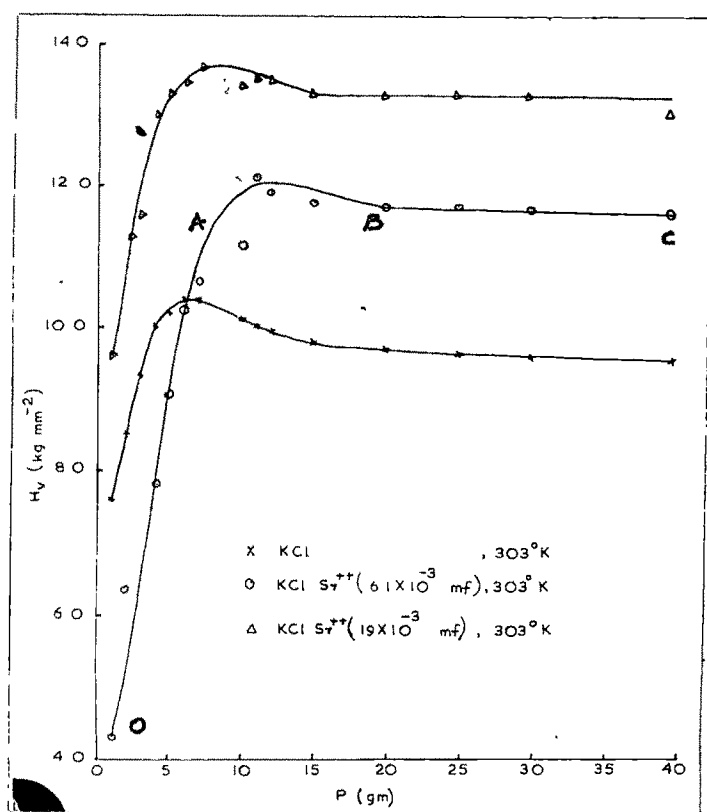
FIG. 11·2
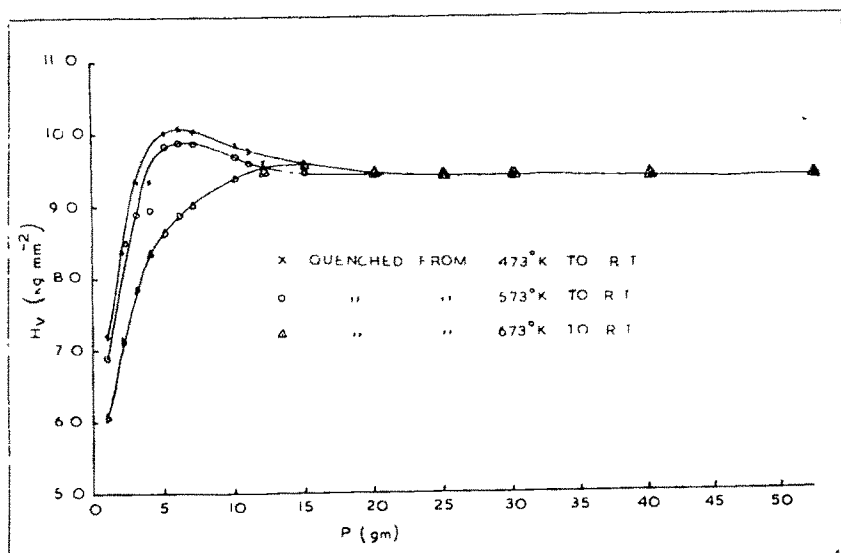
FIG. 11·2
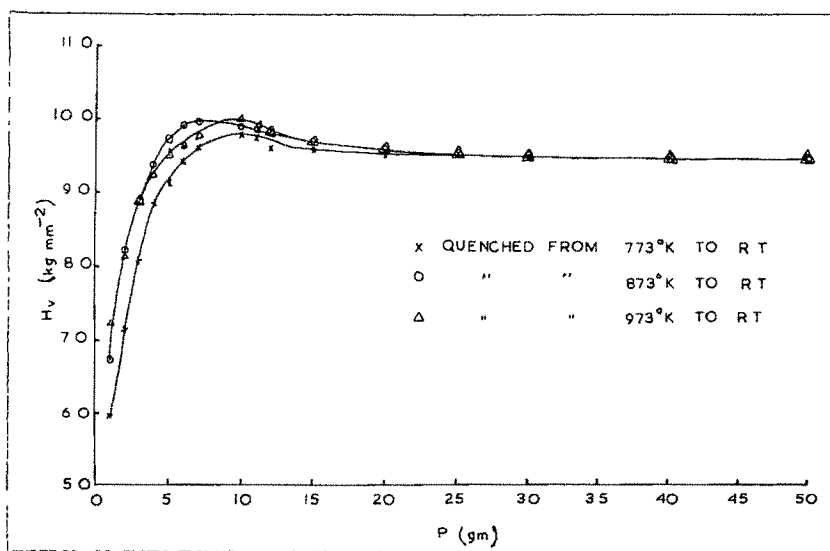
FIG. 11·2

11.3.2 Variation of microhardness with load:

The Vickers hardness numbers are determined
from the observations recorded in Table 11.1 and
microhardness variation is graphically studied from plots
of hardness vs load (Fig.11.2). From the previous study
on the variation of hardness with load for natural calcite
crystals and from a study of the present plots, the
following conclusions are drawn:-

(1) For thermally treated and untreated samples
     (crystals), the graph between hardness and
     load consists of three parts - linear, non-
     linear and linear portions.

(2) The hardness values of quenched samples
     (of KCl crystals) for low loads do not show
     any significant difference from the corres-
     ponding values of untreated samples at room
     temperature; this is also true for medium
     loads. However for high loads the hardness
     is constant and independent of quenching
     temperatures.

(3) For low and medium loads hardness depends
     on temperature.

Quenching temp. °K	P(gm) and H_v(kg.mm^{-2})	Linear (OA)		Non-linear (AB)		Linear (BC)	
		Calcite	KCl	Calcite	KCl	Calcite	KCl
303	P	1-5	1-4	5-50	4-20	50-100	20-50
	H_v	116-150	7.6-10	150-128	10-9.6	128-119	9.6-9.5
473	P	1-6	1-3	6-50	3-20	50-100	20-50
	H_v	116-166	7.2-9.3	116-132	9.3-9.5	132-124	9.5-9.5
573	P	1-3	1-4	3-50	4-15	50-100	15-50
	H_v	140-165	6.9-9.4	165-132	9.4-9.5	132-132	9.5-9.5
673	P	1-5	1-4	5-50	4-20	50-100	20-50
	H_v	152-211	6-8.3	211-154	8.3-9.5	154-144	9.5-9.5
773	P	1-4	1-4	4-40	4-20	40-100	20-50
	H_v	132-190	5.9-8.7	190-148	8.7-9.5	148-132	9.5-9.5
873	P	—	1-3	—	3-20	—	20-50
	H_v	—	7.2-8.8	—	8.8-9.5	—	9.5-9.5
973	P	—	1-4	—	4-20	—	20-50
	H_v	—	6.7-8.8	—	8.8-9.5	—	9.5-9.5
303 Sr^{++}(low)	P	—	1-7	—	7-20	—	20-50
	H_v	—	4.3-10.6	—	10.6-11.7	—	11.7-11.6
303 Sr^{++}(high)	P	—	1-4	—	4-15	—	15-50
	H_v	—	9.6-11.7	—	11.7-13.3	—	13.3-13.3

Range of applied loads (P) and hardness number (H_v) for H_v vs P plots showing three parts

In order to bring out subtle differences
between the behaviour of these (KCl and $CaCO_3$) crystals
which were given identical heat treatment a table is
prepared showing approximately the characteristic ranges
of applied loads (P gm) and hardness (Vickers hardness
numbers, H_v kg/mm^2) for three different regions of the
graph of H_v vs P, viz., linear, non-linear and linear
portions (Table 11.7). In addition to the conclusions
mentioned above, a careful study of this table reveals
the following:-

(a)   For the first region (linear) of the graph the
        range of applied loads for calcite is greater
        than that for KCl; hardness numbers of calcite
        exhibit a very large range of values compared
        to that of KCl. For identical loads, H_v is
        approximately 10 to 20 times more for calcite
        than for KCl. Further hardness number of calcite
        in general increases with quenching temperature
        except for 773°K where it registers a lower
        value and range. This indicates the onset of
        dissociation of calcite at this temperature.
        Hardness numbers for KCl crystals show a little
        variation towards decreasing side so far as the
        range and value are concerned. However there

does not appear to be any consistancy in the
changing values of hardness numbers with quenching
temperatures.

(b)   The range of applied loads in the non-linear range
of the graph is more for both crystals. The
hardness numbers of calcite exhibit a downward
trend in their values with increasing load and
increase with quenching temperature, whereas
irregular fluctuations in their values are observed
for KCl. This suggests that Vickers hardness
number (VHN) changes with load and temperature of
quenching.

(c)   For the third region (linear part) of the graph,
hardness of calcite crystals in general increases
with quenching temperature at a constant indentation
load. This is, however, not true for KCl crystals
for which VHN has practically a constant value for
all loads and quenching temperatures.

(d)   For doped KCl crystals, the first region exhibits
a behaviour which has a close resemblance with that
of calcite at low loads. However the behaviour at
medium and high loads is noticeably different from
that of calcite; VHN increases with increasing load

at medium loads and is constant at high loads.
This is in sharp contrast with the hardness
of pure KCl crystals, where VHN decreases with
increasing load and attains a constant value.

The effect of impurity on hardness was studied
by several workers (e.g. see Matkin and Caffyn (1963),
Dryden et al. (1965), Urusovskaya et al. (1969),
Takcuchi and Kitano (1971)). Temperature dependence of
microharndess was studied by Sarkozi and Vinnay (1971).
They concluded that besides thermal stress the observed
hardening may be due to dislocations piled-up at various
impurities, to complexes in solid solution and vacancy
clusters which were developed at high temperature and by
quenching the clusters became distributed in the crystal
as fine dispersions. The present study suggests that
structure and impurity appreciably influence the hardness
of KCl and $CaCO_3$ crystals. The major contribution to
hardness in the present case appears to be due to impurity
in the crystal. Thermal treatment affects the distribution
of impurities of various types and induces changes in
hardness of crystals (Calcite). The present study is
unable to throw light on how the pinning of dislocations
at various impurities, complexes, vacancies and their

aggregates takes place. It has removed the erroneous impression created from a study of the variation of load with average diagonal length of indentation mark, viz., second part of the graph of logd vs logP is due to structure insensitive property of crystals (cf. see page 151). The hardness study has indicated different behaviour of crystals indented by low, medium and high loads and qualitatively suggested different types of interactions between point defects, aged dislocations in grown crystals and dislocations freshly introduced by indentation. The distribution of dislocations around an indentation mark was studied by many workers (e.g. see Urusovaskaya and Tyagaradzhan (1965), Shukla and Murthy (1968)). The importance of different regions of the graph between hardness and load is not yet clearly quantitatively understood in terms of the defect structure of crystals.

11.3.3 Electrical conductivity of pure and doped KCl crystals:

Ionic conductivity of alkali halides in general and of potassium chloride in particular is studied in much more details and hence comparatively extensive and precise data exist for these crystals. They are now available in standard books on solid state physics (e.g. see, Levy (1968), Dekker (1967), Van Buren (1960)).

T	KCl		KCl:Sr^{++}(6.1x10^{-3})m.f.		KCl:Sr^{++}(19x10^{-3}) m.f.		$\dfrac{10^3}{T}$
	σ	log σT	σ	log σT	σ	log σT	
483	6.699×10^{-11}	$\overline{8}.5099$	–	–	–	–	2.070
493	8.134×10^{-11}	$\overline{8}.6031$	–	–	–	–	2.028
498	–	–	–	–	1.053×10^{-8}	$\overline{6}.7198$	2.008
513	1.294×10^{-10}	$\overline{8}.8221$	–	–	1.949×10^{-8}	$\overline{5}.0000$	1.949
528	–	–	4.910×10^{-9}	$\overline{6}.4137$	2.574×10^{-8}	$\overline{5}.1333$	1.894
533	3.163×10^{-10}	$\overline{7}.2269$	–	–	–	–	1.876
543	–	–	6.900×10^{-9}	$\overline{6}.5746$	4.685×10^{-8}	$\overline{5}.4055$	1.842
553	5.176×10^{-10}	$\overline{7}.4567$	–	–	–	–	1.808
558	–	–	1.116×10^{-8}	$\overline{6}.7942$	9.931×10^{-8}	$\overline{5}.7436$	1.792
563	6.327×10^{-10}	$\overline{7}.5517$	–	–	–	–	1.776
573	8.760×10^{-10}	$\overline{7}.7007$	1.964×10^{-8}	$\overline{5}.0514$	1.528×10^{-7}	$\overline{5}.9423$	1.745
583	1.238×10^{-10}	$\overline{7}.8584$	–	–	–	–	1.715
588	–	–	3.386×10^{-8}	$\overline{5}.2991$	2.482×10^{-7}	$\overline{4}.1643$	1.701
593	1.898×10^{-9}	$\overline{6}.0514$	–	–	–	–	1.686
603	1.669×10^{-9}	$\overline{6}.0028$	4.166×10^{-8}	$\overline{5}.4000$	3.311×10^{-7}	$\overline{4}.3002$	1.658
618	2.564×10^{-9}	$\overline{6}.2000$	5.117×10^{-8}	$\overline{5}.5000$	4.485×10^{-7}	$\overline{4}.4428$	1.618
633	3.698×10^{-9}	$\overline{6}.3693$	7.057×10^{-8}	$\overline{5}.6500$	4.794×10^{-7}	$\overline{4}.4821$	1.580

TABLE 11.4 (contd.)

T	KCl		KCl:Sr^{++}(6.1x10^{-3}) m.f.		KCl:Sr^{++}(19x10^{-3}) m.f.		$\dfrac{10^3}{T}$
	σ	$\log \sigma T$	σ	$\log \sigma T$	σ	$\log \sigma T$	
648	—	—	9.736×10^{-8}	$\bar{5}.8000$	9.268×10^{-7}	$\bar{4}.7786$	1.543
663	7.117×10^{-9}	$\bar{6}.6738$	1.364×10^{-7}	$\bar{5}.9563$	1.121×10^{-6}	$\bar{4}.8712$	1.508
678	—	—	1.857×10^{-7}	$\bar{4}.1000$	1.695×10^{-6}	$\bar{3}.0605$	1.475
693	1.1390×10^{-8}	$\bar{6}.8972$	2.566×10^{-7}	$\bar{4}.2500$	1.782×10^{-6}	$\bar{3}.0916$	1.443
708	—	—	3.162×10^{-7}	$\bar{4}.3500$	2.623×10^{-6}	$\bar{3}.2689$	1.412
723	1.963×10^{-8}	$\bar{5}.1521$	3.273×10^{-7}	$\bar{4}.3741$	3.468×10^{-6}	$\bar{3}.4002$	1.383
738	—	—	5.456×10^{-7}	$\bar{4}.6050$	4.634×10^{-6}	$\bar{3}.5341$	1.355
753	3.163×10^{-8}	$\bar{5}.3770$	7.340×10^{-7}	$\bar{4}.7484$	5.675×10^{-6}	$\bar{3}.6308$	1.328
768	—	—	7.794×10^{-7}	$\bar{4}.7772$	6.952×10^{-6}	$\bar{3}.7275$	1.302
783	5.475×10^{-8}	$\bar{5}.6322$	1.043×10^{-6}	$\bar{4}.9123$	8.387×10^{-6}	$\bar{3}.8174$	1.277
798	—	—	1.693×10^{-6}	$\bar{3}.1307$	9.931×10^{-6}	$\bar{3}.8990$	1.253
813	1.120×10^{-7}	$\bar{5}.9594$	2.232×10^{-6}	$\bar{3}.2588$	1.030×10^{-5}	$\bar{3}.9229$	1.230
828	—	—	2.619×10^{-6}	$\bar{3}.3362$	1.545×10^{-5}	$\bar{2}.1069$	1.208
843	3.917×10^{-7}	$\bar{4}.5188$	4.005×10^{-6}	$\bar{3}.5285$	1.636×10^{-5}	$\bar{2}.1395$	1.186
858	—	—	4.464×10^{-6}	$\bar{3}.5832$	1.986×10^{-5}	$\bar{2}.2315$	1.166
873	9.521×10^{-7}	$\bar{4}.9203$	9.819×10^{-6}	$\bar{3}.9331$	3.089×10^{-5}	$\bar{2}.4309$	1.145
903	1.423×10^{-6}	$\bar{3}.1091$	—	—	—	—	1.107
933	4.067×10^{-6}	$\bar{3}.5792$	—	—	—	—	1.072
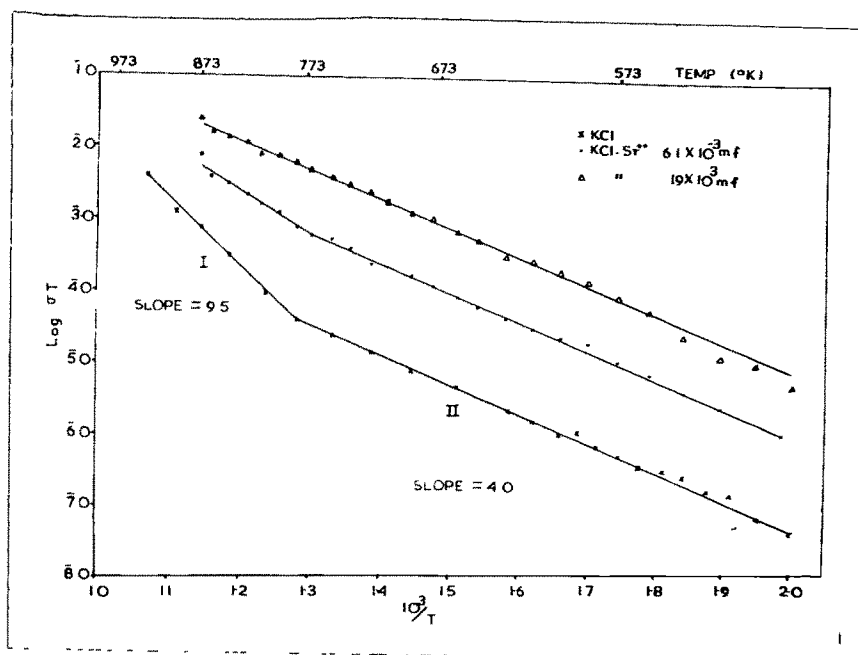
FIG.11·6

TABLE 11.8

Figure	Calcite Temperature		KCl Temperature	
	High	Low	High	Low
$\log H_V$ vs $\log T$		0.35 (1 gm) 0.30 (2 gm)		0.10 (1 gm) 0.025 (2 gm)
$\log H_V T$ vs $\log T$		1.20	1.0	
$\log H_V T$ vs $10^3/T$	0.40	0.16	0.45	0.15
$\log \sigma/H_V$ vs $\log T$	20		16	
$\log Td$ vs $\log T$	0.9		1.0	
$\log \sigma T$ vs $10^3/T$	6.5	4.5	9.5	4.0

S l o p e s

The conductivity of pure and doped KCl crystals at various temperatures is determined in the usual way as described in the previous chapter (page 167). The data is recorded in Table 11.4 and graphical representation is shown in plots (Fig.11.6). The activation energies for the formation and migration of point defects (Schottky defects) are also given in the graph.

11.4 DISCUSSION : (GENERAL)

Since crystals quenched from high temperatures to room temperature show variation in Vickers hardness numbers and the present work on KCl crystals is carried out to support work on calcite and to bring out fine differences, the graphs of (1) $\log H_v$ vs $\log T$ (fig.11.4) (2) $\log H_v T$ vs $\log T$ (fig.11.3) (3) $\log H_v T$ vs $10^3/T$ (fig. 11.5) (4) $\log \sigma/H_v$ vs $\log T$ (fig.11.8) (5) $\log Td$ vs $\log T$ (fig.11.7) and (6) $\log \sigma T$ vs $10^3/T$ (fig.11.6) are plotted for pure KCl crystals. The comparison of these plots with those for calcite (figs. 9.3, 9.2, 9.4, 10.4, 10.3 & 10.2) shows close similarity between them. In order to bring out fine differences between these plots, a table (11.8) is prepared giving the slopes of these graphs for calcite and KCl crystals. The detailed analysis of this table and the plots for calcite and KCl
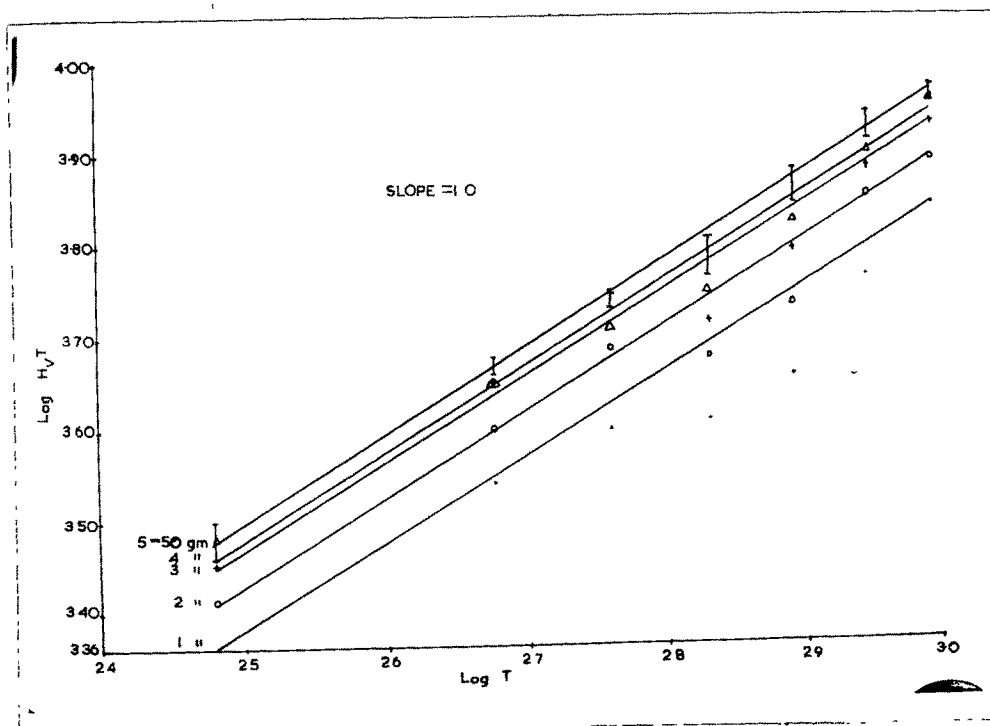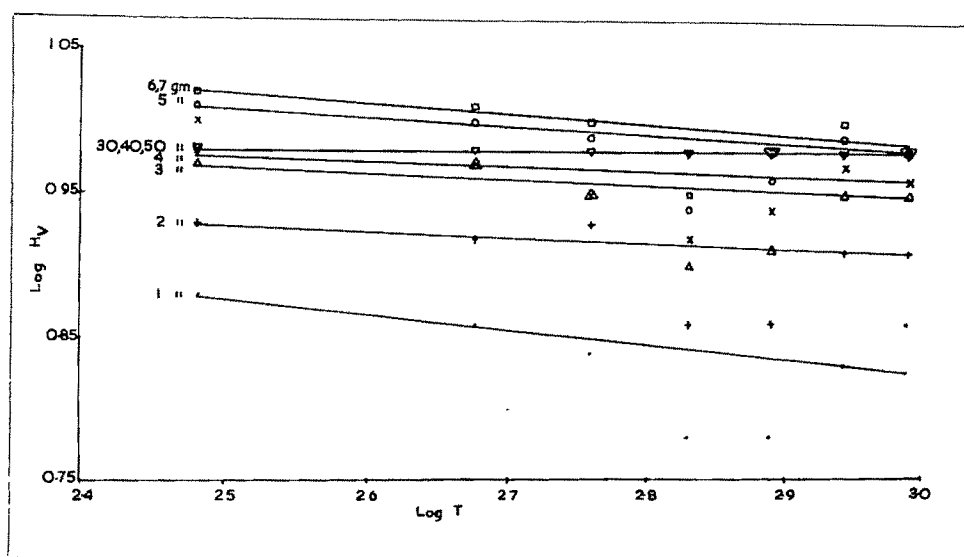
FIG.113

FIG.114

crystals has revealed the following:

(1)   The study of plots of log H_V vs log T for calcite
       (fig.9.3) and KCl (fig.11.4) shows that in the
       former case the dependence of hardness on tempera-
       ture is more prominent than in the latter case.
       The slopes of straight lines for different loads
       are not equal. This shows that applied load is
       an important parameter to be considered in the
       analysis. Further at low loads VHN is more
       influenced by thermal treatment. Gradually this
       dependence reduces with the increase of applied
       loads and particularly for KCl at high loads say,
       30, 40 gm etc.; the hardness is independent of
       temperature.

(2)   The graphs of log H_VT vs log T (fig. 9.2 for
       calcite and fig. 11.3 for KCl) indicate that they
       are better plots than those mentioned above; here
       the scattering of points about a straight line
       is less than for plots of log H_V vs log T. Further
       the straight lines are almost parallel to each other
       for all applied loads. The slopes of parallel
       straight lines are 1.2 and 1.0 for calcite and KCl
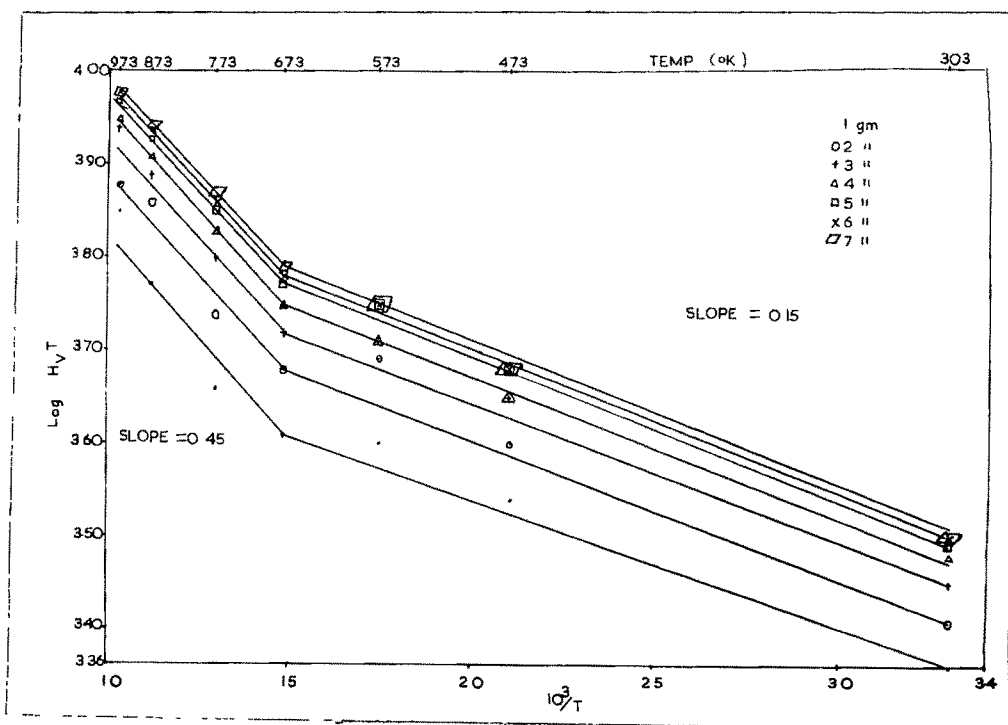   respectively. The higher slope value for calcite

FIG. 11·5

shows that VHN is more sensitive to thermal
treatment of specimens (calcite crystals). The
graph can be fitted into equation $y = cx^b$ where
c and b are constants characteristics of a
straight line. Thus $\log y = \log c + b \log x$.
In the present case y corresponds to $H_v T$ and
x to T. Hence the equation will be $H_v T = cT^b$
or $H_v/c = T^{b-1}$ where b is the slope and c
the intercept on the axis of $\log H_v T$. Since
the value of b is 1.2 (calcite) and 1.0 (KCl),
$H_v/c = T^{0.2}$ (calcite) and $H_v/c = T^{0.0}$ (KCl).
Thus at a constant temperature (H_v/c) is a
constant (3.0 (calcite, 303°K) and 1 (KCl, 303°K))

(3)   The study of graphs of $\log H_v T$ vs $10^3/T$ (fig.9.4
      for calcite and fig. 11.5 for KCl) shows that it
      consists of two straight lines with different
      slopes. At low loads the straight lines are
      parallel to each other. At medium loads this is
      not true and again at high loads (graphs not shown)
      the straight lines are again parallel. This
      supports the conclusions drawn from a study of the
      variation of hardness with load viz., hardness
      behaviour can be divided into three parts - linear,

| P in gm	$\log \dfrac{\sigma}{II}$					
	473°K	573°K	673°K	773°K	873°K	973°K
1	$\overline{13}.9652$	$\overline{11}.0025$	$\overline{10}.3903$	$\overline{9}.3424$	$\overline{8}.0645$	$\overline{7}.3925$
2	$\overline{13}.9008$	$\overline{12}.9123$	$\overline{10}.3171$	$\overline{9}.2569$	$\overline{9}.9452$	$\overline{7}.3424$
3	$\overline{13}.9538$	$\overline{12}.8918$	$\overline{10}.2767$	$\overline{9}.2049$	$\overline{9}.9091$	$\overline{7}.3034$
4	$\overline{13}.9538$	$\overline{12}.8895$	$\overline{10}.2497$	$\overline{9}.1694$	$\overline{9}.8871$	$\overline{7}.2880$
5	$\overline{13}.8230$	$\overline{12}.8480$	$\overline{10}.2350$	$\overline{9}.1529$	$\overline{9}.8731$	$\overline{7}.2742$
6	$\overline{13}.8192$	$\overline{12}.8462$	$\overline{10}.2235$	$\overline{9}.1370$	$\overline{9}.8634$	$\overline{7}.2700$
7	$\overline{13}.8218$	$\overline{12}.8476$	$\overline{10}.2159$	$\overline{9}.1297$	$\overline{9}.8607$	$\overline{7}.2637$
10	$\overline{13}.8295$	$\overline{12}.8550$	$\overline{10}.1970$	$\overline{9}.1206$	$\overline{9}.8634$	$\overline{7}.2519$
11		$\overline{12}.8586$	$\overline{10}.1942$	$\overline{9}.1209$	$\overline{9}.8651$	$\overline{7}.2462$
12		$\overline{12}.8623$	$\overline{10}.1892$	$\overline{9}.1396$	$\overline{9}.8660$	$\overline{7}.2497$
15		$\overline{12}.8687$	$\overline{10}.1850$	$\overline{9}.1303$	$\overline{9}.8721$	$\overline{7}.2551$
20		$\overline{12}.8636$	$\overline{10}.1948$	$\overline{9}.1322$	$\overline{9}.8776$	$\overline{7}.2646$
25		$\overline{12}.8641$	$\overline{10}.1942$	$\overline{9}.1332$	$\overline{9}.8790$	$\overline{7}.2620$
30		$\overline{12}.8641$	$\overline{10}.1942$	$\overline{9}.1338$	$\overline{9}.8798$	$\overline{7}.2627$
40		$\overline{12}.8641$	$\overline{10}.1942$	$\overline{9}.1338$	$\overline{9}.8813$	$\overline{7}.2644$
50		$\overline{12}.8641$	$\overline{10}.1952$	$\overline{9}.1338$	$\overline{9}.8813$	$\overline{7}.2644$
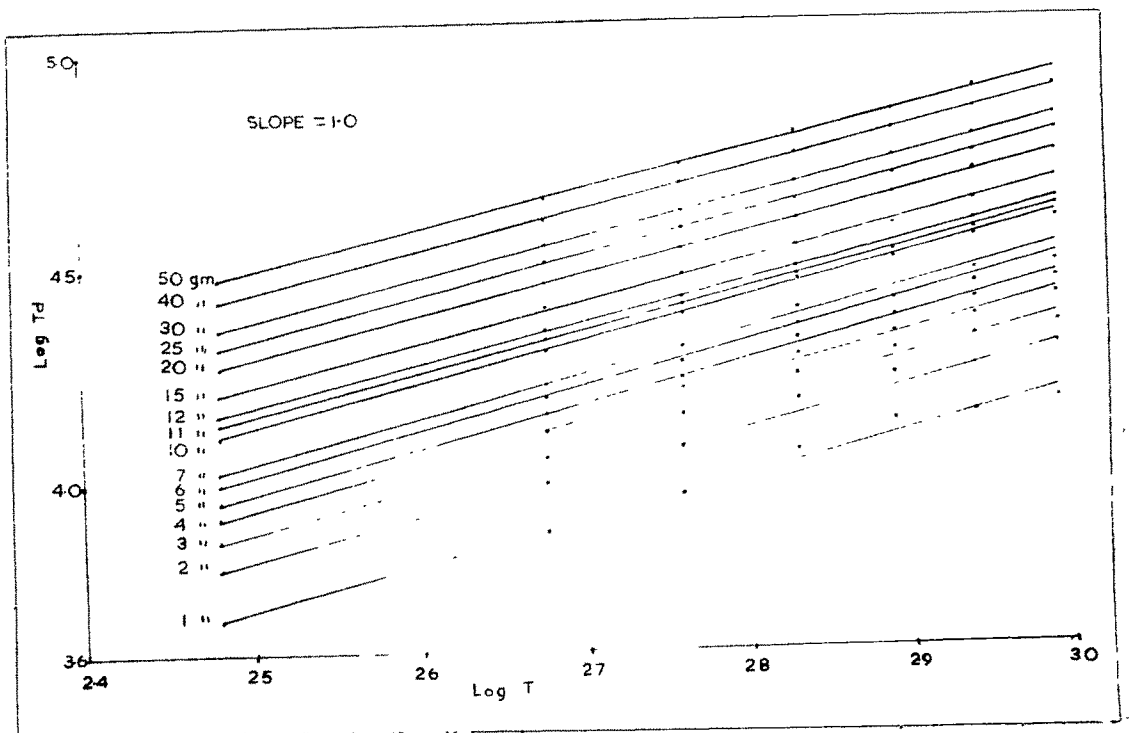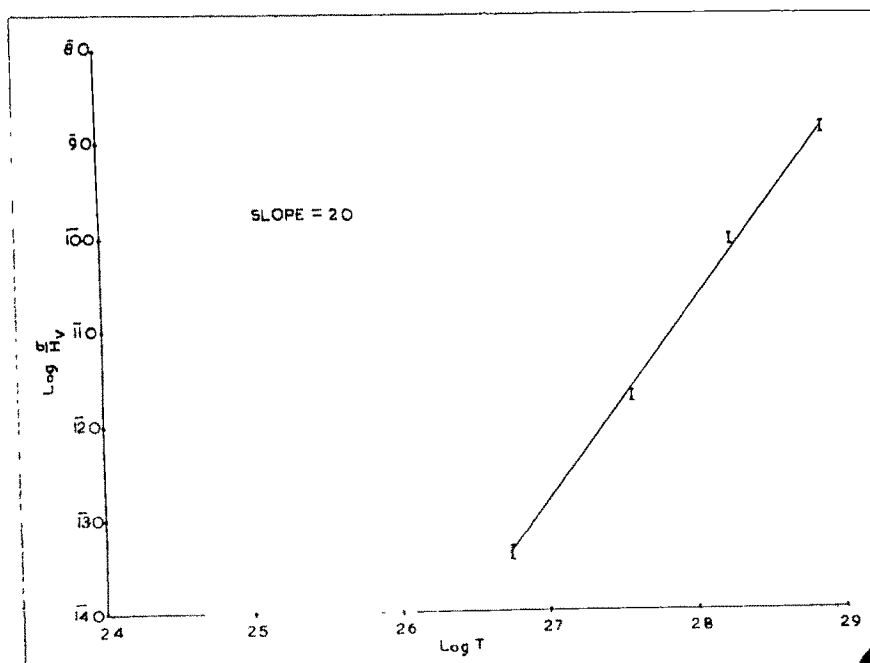
FIG 11.7

FIG. 11.8

non-linear and linear - corresponding to three
ranges of loads, low, medium and high loads.
Assuming the exponential relation between (H_vT)
and $(1/T)$, viz. $H_vT \propto e^{-E/KT}$, it is possible to
calculate the activation energies for the plastic
flow in calcite and KCl crystals. For low quenching
temperatures they are about 0.3 eV for both crystals
whereas for high temperatures the values are 0.8 eV
(calcite) and 0.9 eV (KCl). In view of approximately
equal values it can be conjectured that the mechanisms
operating within these crystals giving rise to these
values are likely to be more or less similar. This
remark requires more critical examination by collecting
and studying data on different crystals. At present
little data is available from literature (cf. Chapter
VII). Edelman (1964) showed exponential dependence
of microhardness of InSb and GaSb single crystals on
temperature and estimated the activation energy for
plastic flow in both these crystals to be 0.6 eV.

(4)   The plots of $\log \sigma/H_v$ vs log T are straight lines
with slopes 20 (fig.10.4) and 16 (fig.11.8) for
calcite and KCl crystals respectively. Unlike the
previous cases (1), (2) and (3), there is only one
straight line in both the cases. This shows that

TABLE c.11

P in gm	logTd						
	303°K	473°K	573°K	673°K	773°K	873°K	973°K
1	3.6752	3.8790	3.9722	4.0712	4.1373	4.1617	4.1923
2	3.8010	3.9970	4.0778	4.1850	4.2452	4.2684	4.3179
3	3.8683	4.0618	4.1562	4.2534	4.3073	4.3389	4.3861
4	3.9169	4.1239	4.2166	4.3014	4.3524	4.3901	4.4409
5	3.9603	4.1574	4.2442	4.3432	4.3916	4.4270	4.4830
6	3.9949	4.1951	4.2810	4.3736	4.4243	4.4663	4.5195
7	4.0302	4.2297	4.3175	4.4119	4.4535	4.4987	4.5503
10	4.1123	4.3109	4.3991	4.4751	4.5266	4.5770	4.6228
11	4.1370	4.3340	4.4210	4.4932	4.5474	4.5978	4.6449
12	4.1547	4.3572	4.4427	4.5103	4.5587	4.6177	4.6648
15	4.2079	4.4051	4.4926	4.5563	4.6125	4.6694	4.7165
20	4.2730	4.4673	4.5532	4.6238	4.6823	4.7351	4.7823
25	4.3226	4.5168	4.6025	4.6731	4.7318	4.7836	4.8309
30	4.3636	4.5564	4.6418	4.7096	4.7718	4.8240	4.8711
40	4.4272	4.6218	4.7051	4.7774	4.8357	4.8886	4.9357
50	4.4760	4.6694	4.7526	4.8253	4.8839	4.9356	4.9827

for a crystal (σ/H_v) is constant at constant
temperature for all applied loads. This law
suggests that point defects which are active
in exhibiting the conductivity property of a
crystal are also involved in some way with the
(cf chapter X)
hardness behaviour of treated crystals. It is
necessary to have the hardness work on different
crystals which in turn will lead to a better
appreciation and interpretation of the proposed
law.

(Fig 10.3 & 11.4)

(5)   The graphs of log Td vs log T consist of a
series of parallel straight lines corresponding
to different applied loads. The spacing between
any two consecutive parallel lines is not constant.
These graphs closely resemble those of log H_vT
vs log T. This also explains the physical fact
that hardness number and diagonal length of inden-
tation mark are intimately connected with each
other. The graph can be fitted into an equation
$y = wx^v$ where w and v are constants of a
straight line. The logarethmic equation will
therefore be log y = log w + v log x. Here y
corresponds to Td and x to T. Hence the equation

is $Td = wT^V$ or $d/w = T^{V-1}$. Hence at constant

temperature, d/w is constant. This ratio is

independent of load. 'w' is the intercept on

the axis of log Td ($d/w = 0.56$ (calcite, 303°K),

$d/w = 1.0$ (KCl, 303°K)).

(6)   From the plots of log σT vs $10^3/T$ (figs. 10.2

& 11.6) the jump activation energy is 0.9 eV

for calcite whereas it is 0.8 eV for 'pure' KCl

crystals. The formation energy for defect pair

is 0.8 eV for calcite and 2.2 eV for KCl crystals.

Electrical properties of non-cubic ionic crystals

are rather less investigated. This is more true

for natural and synthetic calcite crystals which

form a highly complicated system compared to the

cubic system. $NaNO_3$ which is isomorphous to

calcite was studied for ionic conductivity

(Ramsastry and Murti (1968)). Studies of electrical

conduction in pure and doped KCl crystals were

made by many workers (e.g. see Dreyfus and Nowick

(1962), Allnatt and Jacob (1962), Jain and Dahake

(1963, 1964), Fuller (1966), Beaumon and Jacob

(1966), Lidiard (1970)) for obtaining information

concerning the defect solid state. Dr. Lidiard's

article (1957) lucidly summarized the work done

in ionic transport upto about 1957. With the
development of ionic solid state devices,
interest is now renewed with more enthusiasm
to examine in greater detail the existence and
properties of the well established and newly
proposed transport mechanisms (Fuller, 1970).
The present author would not like to touch
these mechanisms as his main interest was to
trace the supporting experimental evidence on
the law, proposed in the present work, pertaining
to the relation between electrical conductivity
and VHN. The conclusions which were drawn from
hardness and conductivity study of calcite were
supported to a greater extent by the work on
KCl crystals.

There is a certain amount of repeatation of text
of the previous chapters in this chapter. This could
not be avoided since the present work was planned with
a twin objective of realizing (1) confirmation of results
on microharndess of calcite crystals and (2) a comparative
study of hardness of natural calcite and synthetic KCl
crystals to bring out subtle differences due to structure
etc. The work on KCl crystals simply supported the

conclusions obtained from a study of microhardness and electrical conductivity of natural calcite crystals.

It should be remarked here that the present approach to the study of microhardness of calcite crystals is essentially phenomenalogical in nature and that work on microhardness of KCl crystals was taken up for the purpose of verifying the general conclusions arrived at from VHN study of calcite crystals. It suffers from a serious disadvantage that the data reported in the present work was for two crystals (calcite and KCl) of different structures. Further not much work of this type is available in literature. Hence the present data is quite inadequate in view of the fact that actual impurity content in both these crystals is not known with certainty. Natural calcite may contain impurities of different types and concentrations. In case of doped KCl crystals, the amount added to the fused charge is known; however the actual amount in a given sample could not be ascertained with certainty due to limitations of laboratory. It is therefore desirable to have an extensive reliable and accurate data on several crystals of identical and different structures. This work is being actively pursued in this laboratory. Besides a model theory is also being developed to account for the dependence of VHN of ionic crystals on several factors including temperature of quenching.